QM/MM STUDY ON THE ELONGATION FACTOR-TU (EF-Tu)

by

Hasan Hüseyin İnce

B.S., Chemistry, Middle East Technical University, 2008

Submitted to the Institute for Graduate Studies in
Science and Engineering in partial fulfillment of
the requirements for the degree of
Master of Science

Graduate Program in Chemistry

Boğaziçi University

2012

QM/MM STUDY ON THE ELONGATION FACTOR-TU (EF-Tu)

APPROVED BY:

Prof. Viktorya Aviyente …….
(Thesis Supervisor)

Assist. Prof. Bülent Balta …….
(Thesis Co-supervisor)

Prof. İlknur Doğan …….

Assoc. Prof. Nurcan Tüzün …….

Assist. Prof. F. Aylin Sungur …….

DATE OF APPROVAL: 30.07.2012

To Reha, Yavuz and Hanzade

ACKNOWLEDGEMENTS

I would like to express my sincere gratitude to my thesis advisor Prof. Viktorya Aviyente for her encouragement and assistance throughout my studies. In addition, I would like to thank to her for her endless patience. It was a great opportunity to study in her group and improve myself thanks to her useful comments and excellent scientific guidance.

I wish to appreciate to the members of my committee: my co-advisor Assist. Prof. Bülent Balta (Istanbul Technical University), Prof. İlknur Doğan (Boğaziçi University), Assoc. Prof. Nurcan Tüzün (Istanbul Technical University) and Assist. Prof. F. Aylin Sungur (Istanbul Technical University) for giving their valuable time and advices.

I would like to thank to all the members of Computational Chemistry Group, Şeref Gül, Berna Doğan, Özlem Karahan, Tuğba Furuncuoğlu, Gülşah Çifci and Sesil Agopcan for their enjoyable company and valuable contributions to my studies and especially to Asli Yildirim for her additional support and friendship. I would also like to thank all my friends especially to Selman Taş and Berk Çamlı and all the members of the Chemistry Department especially to Murat Burak Türk, Fatih Çömert and Ahmet Erdem.

Finally, my deepest thanks go to my family for their continuous support and endless love throughout my life.

ABSTRACT

QM/MM STUDY ON THE ELONGATION FACTOR-TU (EF-Tu)

EF-Tu is a member of the GTP binding protein superfamily which consists of proteins carrying information and biological components in cells. When the ternary complex of EF-Tu:GTP:aa tRNA binds to the ribosome, cognate codon anticodon interaction triggers the fast hydrolysis of the EF-Tu bound GTP. The hydrolysis of GTP leads to a remarkable conformation change in EF-Tu as it returns to the GDP (loose) conformation from its GTP (tight) conformation. This conformational change decreases the affinity of EF-Tu to the ribosome and abolishes its affinity towards the aa-tRNA resulting in the release of EF-Tu:GDP complex from aa tRNA and ribosome. As the hydrolysis of GTP to GDP is of central importance in the functioning cycle of G proteins. Considerable amount of computational and experimental studies were directed to elucidate the mechanism of non-enzymatic phosphate hydrolysis in solution. The main mechanistic debate on GTP hydrolysis or phosphate hydrolysis in general is whether it follows an associative or dissociative pathway. The associative pathway can be described by the formation of an intermediate with a penta-coordinated phosphorus atom whereas the dissociative pathway can be described by the formation of a metaphosphate ion as an intermediate. In our study we will mainly emphasize the GTP conformation of the elongation factor Tu (EF-Tu) and investigate the mechanistic pathways in GTP hydrolysis by using Quantum Mechanical/Molecular Mechanical (QM/MM) approach as a hybrid computational method.

ÖZET

UZAMA FAKTÖRÜ-TU'DA (EF-Tu) GTP HİDROLİZİNİN QM/MM YÖNTEMİ İLE MODELLENMESİ

EF-Tu hücrelerde bilgi ve biyolojik bileşenler taşıyan proteinleri içeren GTP bağlayıcı protein ailesinin bir üyesidir. EF-Tu:GTP:aa tRNA üçlü kompleksi ribozoma bağlandığı sırada eşasıllı kodon ve antikodon etkileşimi GTP bağlı EF-Tu'da hızlı hidrolizi tetiklemektedir. GTP hidrolizi, GTP (sıkı) konformasyonundan GDP (gevşek) konformasyonuna dönerken EF-Tu'da dikkate değer konformasyon değişikliklerine yol açmaktadır. Bu konformasyon değişikliği EF-Tu'nun ribozoma bağlanma eğilimini azaltmakta ve aa-tRNA'ya olan bağlanma eğilimini ortadan kaldırarak EF-Tu:GDP kompleksinin aa-tRNA ve ribozomdan ayrılmasına yol açmaktadır. GTP'nin GDP'ye hidrolizi G-proteinlerin işleyiş döngüsünde büyük önem arz ettiği için birçok deneysel ve hesaplamalı çalışma, çözelti içerisindeki enzimatik olmayan fosfat hidrolizi üzerine gerçekleştirilmiştir. GTP hidrolizi ya da genel olarak fosfat hidrolizi hakkında asıl mekanistik tartışma asosyatif ve disosyatif yollardan hangisini izlediği üzerine olmuştur. Asosyatif mekanizma penta-koordine fosfor atomlu bir ara ürün oluşumu olarak tanımlanabilir. Disosyatif mekanizma ise ara ürün olarak meta-fosfat iyonu oluşumu olarak tanımlanabilir. Bu çalışmada genel olarak uzama faktörü-Tu'nun GTP konformasyonu üzerinde durulmuş ve GTP hidrolizindeki mekanistik yollar bir hibrit hesaplama yöntemi olan Kuantum Mekanik/Moleküler Mekanik (QM/MM) yaklaşımı ile incelenmiştir.

TABLE OF CONTENTS

LIST OF FIGURES

LIST OF TABLES

LIST OF SYMBOLS

a	Accelaration
B_{ij}	Coulomb potential
D	Number of atoms in the system
E	Potential energy
E_b	Energy for bond angle
E_{nb}	Energy for non-bonded interactions
E_s	Energy for bond stretching
E_ω	Torsional energy
F	Force
F(k)	Force vector
f(r)	Conservative force acting on the particle
f′	Random force
h	Planck's constant
k_b	Boltzmann constant
k^b	Force constant for bending
k^s	Force constant for strectching
l	Actual bond length
l_0	Assigned bond length
M	Total number of bond angles
m	Mass
N	Total number of bonds
p	Momentum
q	Phase point
q_i	Partial charge on atom i
q_j	Partial charge on atom j
r_{ij}	Distance between atom i and j
T	Absolute temperature
x	Position vector in 3N dimensional space
γ	Phase factor

ε	Dielectric constant of medium
ζ	Frictional constant
θ	Actual bond angle
θ_0	Assigned bond angle
$\lambda(k)$	Step size
ω	Torsion angle

LIST OF ACRONYMS/ABBREVIATIONS

aa	Amino acid
aa-tRNA	Amino acyl-tRNA
Ala	Alanine
Arg	Arginine
Asn	Asparagine
Asp	Aspartate
ATP	Adenosine triphosphate
Cys	Cysteine
E.coli	Escherichia Coli
EF-Tu	Elongation Factor-Tu
GAP	GTPase activating protein
GBP	GTP binding protein
GDP	Guanosine diphosphate
GEF	GTP/GDP exchange factor
Gln	Glutamine
Glu	Glutamate
Gly	Glycine
GTP	Guanosine triphosphate
GTPase	GTP hydrolyzing enzyme
His	Histidine
Ile	Isoleucine
Leu	Leucine
Lys	Lysine
MD	Molecular dynamics
Met	Methionine
mRNA	Messenger ribonucleic acid
PDB	Protein data bank
PMEMD	Particle mesh ewald molecular dynamics
Phe	Phenylalanine
Pro	Proline

Ser	Serine
T. Aquaticus	Thermus Aquaticus
T. Thermophilus	Thermus Thermophilus
Thr	Threonine
Trp	Tryptophan
Tyr	Tyrosine
tRNA	Transfer ribonucleic acid
Ts	Temperature stable
Tu	Temperature unstable
UFF	Universal Force Field
Val	Valine

1. INTRODUCTION

Ribosome requires external protein factors including several guanosine 5'-triphosphate (GTP)-hydrolyzing enzymes known as GTPases in all stages of protein synthesis. These highly conserved and essential proteins include elongation factor Tu (EF-Tu)for delivering the aminoacyl-tRNA to the ribosome as a part of a ternary complex with GTP. Other proteins involved in the ribosomal protein synthesis are the elongation factor G and initiation factor 2 [1].

EF-Tu is a G-protein. A common property of G-proteins is cycling between active and inactive conformations depending on the bound nucleotide which can be either GTP (active) or GDP (inactive). Upon matching of codon and anticodon, GTP is hydrolyzed to GDP and this change comes with an extensive conformational change in EF-Tu. As a result of this conformational change, EF-Tu dissociates from the ribosome by transferring aminoacyl-tRNA to the ribosome [2]. Intrinsic GTPase activity of EF-Tu is observed to be very slow ($< 10^{-5}$ s^{-1}) when compared to the most other G-binding proteins [3]. EF-Tu'sGTPase activity is mainly affected by the programmed ribosome causing a 10^7-fold increase in activity [4]. Although more attention was paid to intrinsic GTPase activity starting from the last half of 1980s till to the beginning of 1990s [5], the main concern became GTP hydrolysis mechanism after mid-1990s.

1.1. Functional Studies of EF-Tu in the Presence of Ribosome

Pre-steady state kinetic studies [6] and single-molecule techniques [7] have allowed the analysis of the elongation phase into a number of discrete steps (Figure 1.1) with the application of different fluorescent and radioactive probes. The elongation cycle is divided into three sections as aa-tRNA selection, peptide bond formation, and translocation, which are controlled by EF-Tu, 23S rRNA of the large ribosomal subunit assisted by the 3′ terminal 2′-OH group of P site-bound tRNA [8], and EF-G [9] respectively. In particular, the decoding process has also been divided into subsections as initial binding of the ternary complex, codon−anticodon recognition, GTPase activation, GTP hydrolysis, Pi release, and A site accommodation of the aatRNA (Figure 1.1).

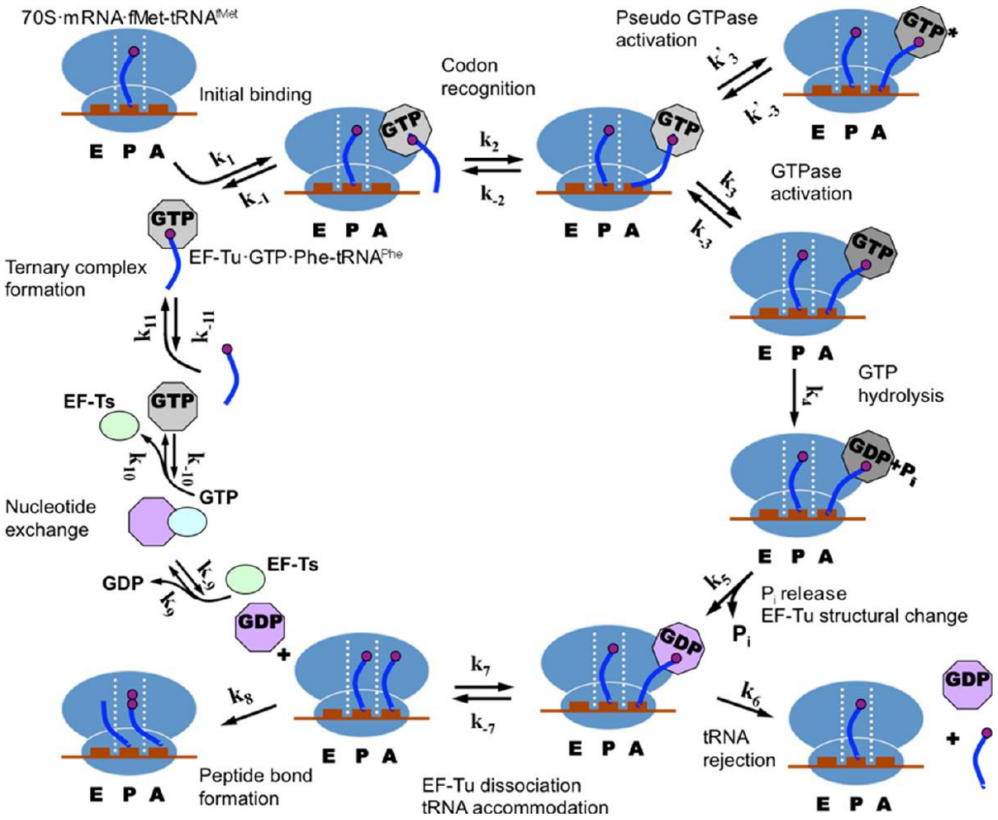

Figure 1.1. Functional cycle describing the kinetic steps of EF-Tu as defined by pre-steady kinetics and/or single-molecule FRET studies [10].

Initial binding is a reversible reaction (Figure 1.1, step 1) independent of the codon subjected to the A site. In the same way, the ribosomal site of initial binding does not overlap with the A site [11]. In addition, the subsequent step of codon recognition is reversible (Figure 1.1, step 2) but may lead to GTPase activation (Figure 1.1, step 3) in case a proper codon−anticodon interaction is achieved. GTPase activation is substantially faster (approximately 100−1000 times) for cognate tRNA species than for near-cognate species [12-14]. Also, noncognate ternary complexes may be rejected at this point without triggering GTP hydrolysis. The cognate conformational alterations linked with the codon−anticodon recognition result in the proper positioning of the catalytic machinery and let the chemical step of GTP hydrolysis (Figure 1.1, step 4). The cleaved-off γ-phosphate is then released and consequently the conformational switch of EF-Tu occurs (Figure 1.1, step 5). Dissociation of P_i seems to limit the rate of the structural rearrangement of EF-Tu into its inactive GDP-bound conformation [15]. As a result of the

structural transition, the factor looses its affinity for the aa-tRNA and the ribosome, thus dissociates (Figure 1.1, step 7). In this way, the aa-tRNA is thereby set free to fully accommodate in the ribosomal A site, whereafter the peptide bond formation can occur (Figure 1.1, step 8). Step 8, like the step of GTPase activation, is accelerated in the case of cognate tRNAs [12] As an alternative, the aa-tRNA may be rejected at this point (Figure 1.1, step 6). The spontaneous dissociation of GDP is very slow (0.001 s^{-1}) and so reactivation of EF-Tu after amino acid delivery is stimulated by its guanine exchange factor EF-Ts [16]. Exchange of guanine nucleotide takes place via the formation of a labile EF-Tu·GDP·EF-Ts complex from which GDP dissociates (Figure 1.1, step 9). The eventuating binary complex is stable but can bind GTP or rebind GDP and dissociate into EF-Tu·GTP upon release of EF-Ts (Figure 1.1, step 10).

In summary, two possibilities arise during the sequence of events which point out two possibilities of aa-tRNA selection occurring based on their different stabilities on the ribosome [17]. The first possibility is defined as "initial selection" and occurs before the GTP hydrolysis (Figure 1.1, reverse of step 2) and on the other side the second option occurs later and is termed as "proofreading" (Figure 1.1, step 6).

1.2. Structural Studies of EF-Tu in the Absence of Ribosome

EF-Tu and its eukaryotic counterpart (EF-1α) is a monomeric protein with about 400 amino acids, and a molecular mass of 40-52 kDa. It consists of three domains known as, Domain I (aa: 1-212), Domain II (aa: 212-310) and Domain III (310-405). Domain I includes the nucleotide binding site, therefore it is also called G-domain [18-20].

The G-domain is recognized as a common building block for GDP/GTP binding in all G-binding proteins and the G-domain of EF-Tu found to contain consensus sequences I [GxxxxGK(S/T); E. coli EF-Tu G_{18}HVDHGKT_{25}, "P-loop"], II (DxxG; E. coli EF-Tu D_{80}CPG_{83}), and III (NKxD; E. coli EF-Tu N_{135}KCD_{138}**)** in addition to SAL motif (E. coli EF-Tu $S_{173}AL_{175}$) [21]. The effector region in EF-Tu is part of the polypeptide chain between helix A (residues 24-35) and β strand b (residues 62-72). The C-terminal part of the effector region of EF-Tu-GDP is a β hairpin and in EF-Tu-GTP complex, this region forms an α helix [19]. Sequences I and II with the effector region, a Mg^{2+} ion and water

molecules coordinate the phosphate groups of the nucleotide while sequence III and SAL motif interact with guanine base. Switch I (residues 51-62) and switch II (residues 82-97) regions are located in domain I and have great importance to observe certain conformational changes during GTP – GDP cycling. The structures of EF-Tu from two thermophilic bacteria have been revealed in their active conformation bound to the nonhydrolyzable GTP analogue, GDPNP [18, 22]. When compared to its inactive form from E. coli [23], structures revealed a dramatic change in domain I when compared to domain II and domain III with the disappearance of the central hole observed in the inactive form. In active form, switch I consists of two α-helices and one of these helices turns to a β-sheet in inactive form. During this cycling, one α-helical turn on switch II unwinds at the C-terminus and a new one is formed in the N-terminus. These structural changes can be seen on Figure 1.2 and Figure 1.3 where switch I has yellow and switch II has magenta color.

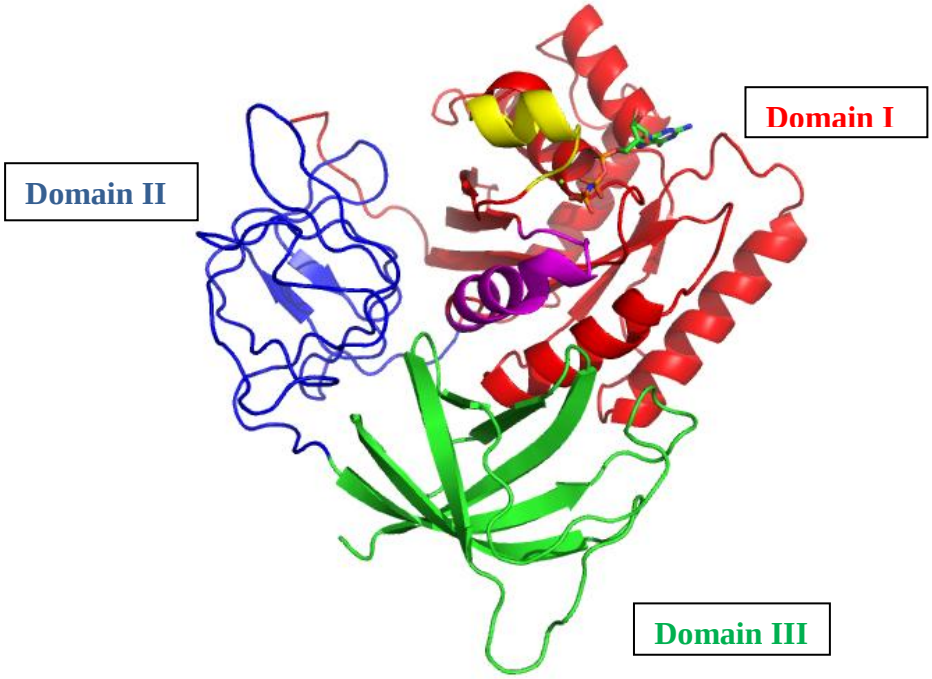

Figure 1.2. Structure of GTP bound EF-Tu in its active form (PDB ID: 1EFT).

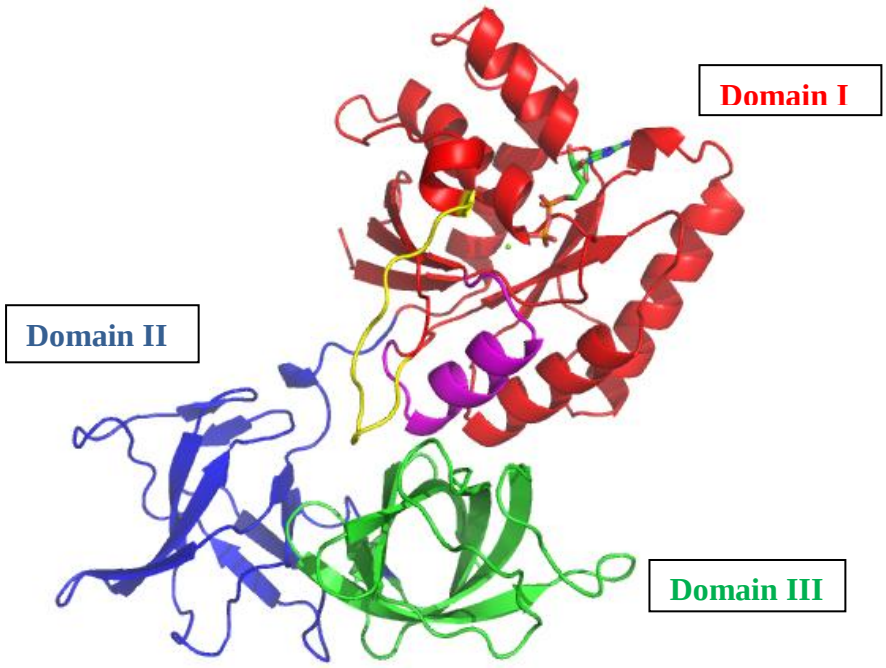

Figure 1.3. Structure of GDP bound EF-Tu in its inactive form (PDB ID: 1TUI).

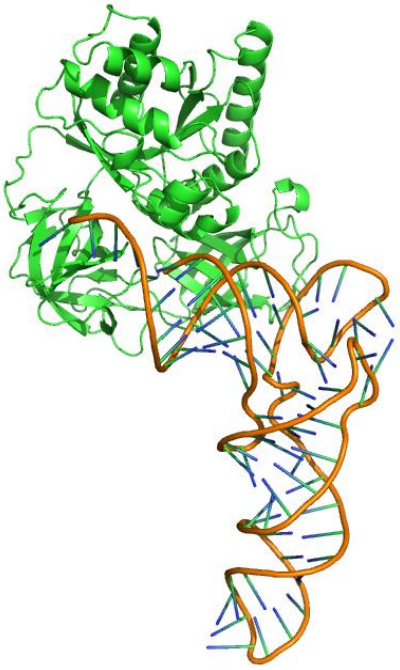

Figure 1.4. EF-Tu·GDPNP·Phe-tRNAPhe ternary complex (PDB ID: 1TTT).

In 1995, the structure of the ternary complex, EF-Tu·GDPNP·Phe-tRNA^{Phe}was clarified (Figure 1.4) [24]. According to this breakthrough, aminoacylated CCA-3' end was found to bind in a pocket formed between domain I and domain II of EF-Tu whereas part of the acceptor stem binds to domain III. In another study,Cys-tRNA^{Cys} containing structure of the ternary complex was determined. This structure was similar to the ternary complex with Phe-tRNA^{Phe}, suggesting that mode of aa-tRNA binding was universal [25].

Another breakthrough was made with the determination of complex structure between EF-Tu and EF-Ts from two different species (Figure 1.5). These studies revealed that EF-Ts binds through domain I and domain III of EF-Tu. Specifically, a phenylalanine residue (Phe81) from EF-Ts was found to intervene between two histidine residues (His85 and His118) positioned at domain I of EF-Tu. Upon comparison of EF-Tu·GDP and EF-Tu·EF-Ts crystal structures, it is suggested that displacement of His118 residue would release the β-phosphate of GDP in the course of the displacement of His85 in the switch II region would disrupt the Mg^{2+} binding site [26, 27].

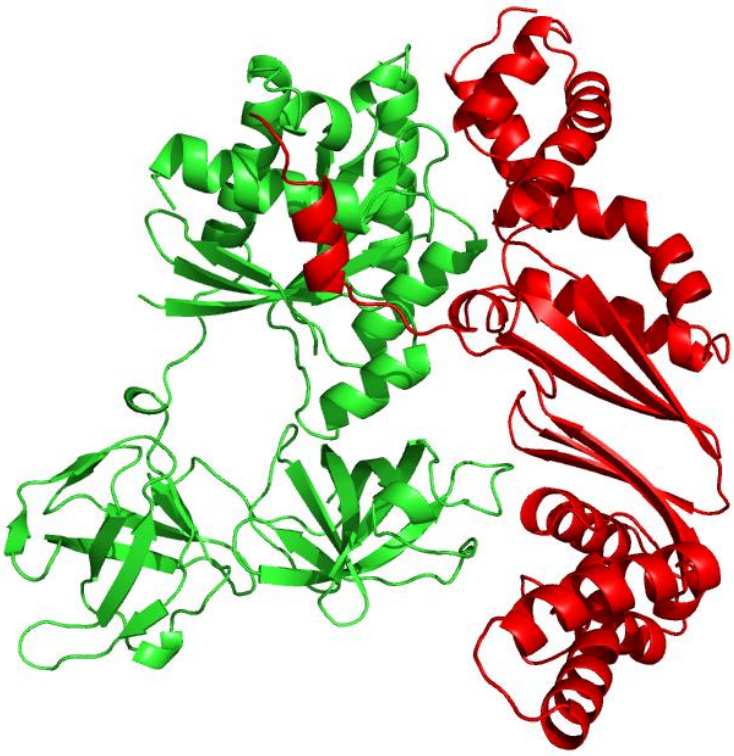

Figure 1.5. EF-Tu·EF-Ts complex (PDB ID: 1EFU).

1.3. Structural Studies of EF-Tu in the Presence of Ribosome

The first ternary complex structure on the ribosome was reported in 1997 [28] showing that the amino acyl end of the aa-tRNA molecule was bound to EF-Tu and the anticodon end was found to interact with the decoding center of the small ribosomal subunit. Later, studies revealed that the occupation of this state required the tRNA to bend and twist allowing its concurrent binding to the mRNA codon and EF-Tu [29]. It has been suggested that this is a universal mechanism of aa-tRNA testing [30], and EF-Tu is proposed to assure that all aa-tRNAs are introduced in the same way to the ribosome.

In 2000, first high-resolution structures of the 30S [31] and 50S [32] subunits were reported. Following this, the structure of the 70S complex with mRNA and tRNAs bound in the A, P, and E sites was published [33]. The 30S subunit during decoding was imaged throughX-ray studies and it was revealed that bases in 16S rRNA, namely G530, A1492, and A1493 (Figure 1.6) are highly conserved and these bases are suggested to monitor the formation of correct Watson−Crick base pairs at the first and second codon positions by forming hydrogen bonds inside the minor cavity of a correctly formed base pair presenting a characteristic stereochemical geometry [34].

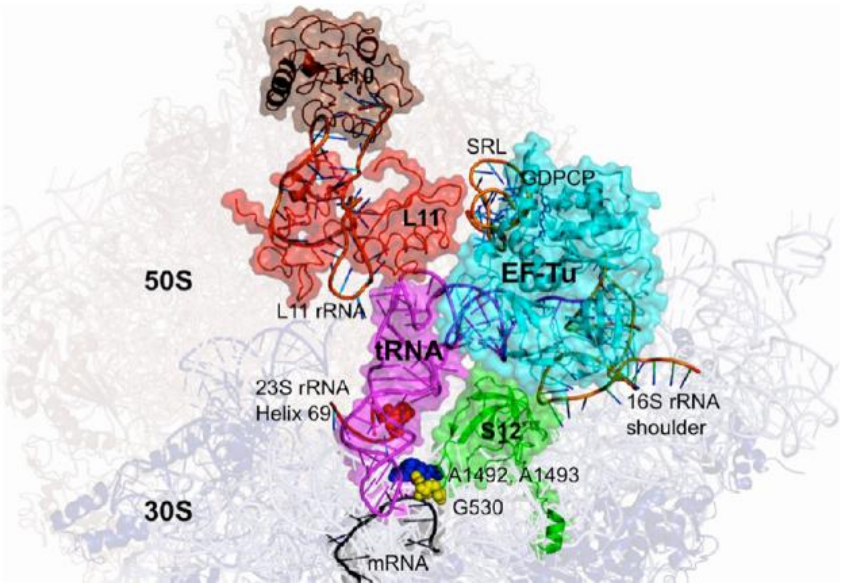

Figure 1.6. Structure of the ternary complex EF-Tu·GDPCP·Trp-tRNATrp bound to the 70S ribosome [10].

Recently, in the presence of the antibiotic paramomycin, the crystal structure of EF-Tu·GDPCP·Trp-tRNA^{Trp} bound to the 70S ribosome was reported and shed light on the structural rearrangements which result in transmitting the signal of cognate codon−anticodon interaction to the GTPase center of EF-Tu [35]. Within this study, it is shown that catalytic His85 and the 5′ end of tRNA is altered, while the contact between the switch I region of EF-Tu containing Ile60 and tRNA 3' end is abolished [35]. The side chain of His85 is oriented away from the active site in the absence of the ribosome whereas it is in the active site in the presence of ribosome. Orientation of His85 into its catalytic conformation by the phosphate group of A2662 of the SRL (Sarcin-Ricin Loop) in 23S rRNA is concluded to lead the conformational changes specified above (Figure 1.7, panels A and B) and His85 has been suggested to serve as a general base in order to deprotonate the catalytic water molecule to initiate its nucleophilic attack to the γ-phosphate of GTP. Following GTP hydrolysis, the cleaved-off γ-phosphate is suggested to be released leading to the disorder of the switch I region and to the rotation of His85 into its inactive state where it is proposed to be stabilized through an interaction with the 2′-OH group of G2661 of the SRL (Figure 1.7, panel C) [29].

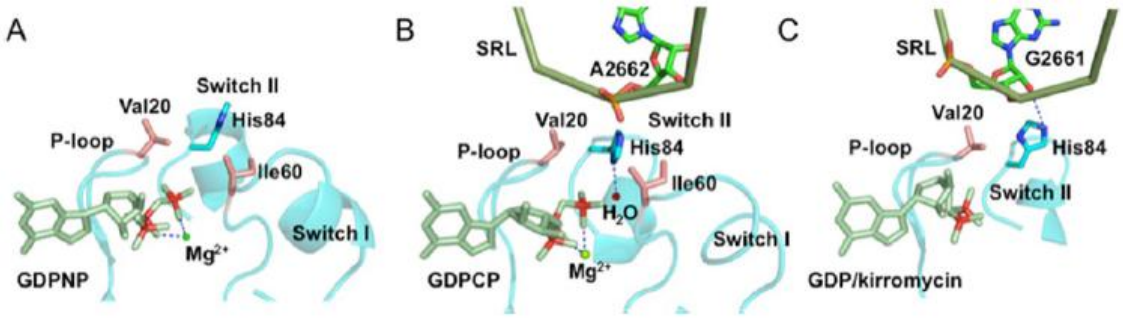

Figure 1.7. Snapshots of the GTP binding site of EF-Tu illustrating the structural changes accompanying GTPase activation and GTP hydrolysis [10].

Another important point regarding the His85 activity is that there are two other important residues in EF-Tu, namely the valine 20 (V20) and isoleucine 60 (I60). In structures of EF-Tu·GTP complex, His85 points away from the catalytic site and its access to the GTP and hydrolytic water molecule is hindered by the side chains of Val20 and Ile60 that form a hydrophobic gate (Figure 1.8). It was suggested that, in order to catalyze the GTP hydrolysis, in the presence of the ribosome, one or both wings of the hydrophobic

gate could open, providing access of His85 to the γ-phosphate [5]. However, neither mutation valine to glycine (V20G) nor isoleucine to alanine (I60A) increased the GTPase activity [36, 37]. Moreover, the crystal structure in the presence of the ribosome shows that the conformations of these residues undergo minor changes, suggesting that this may not seriously affect the GTP hydrolysis [35].

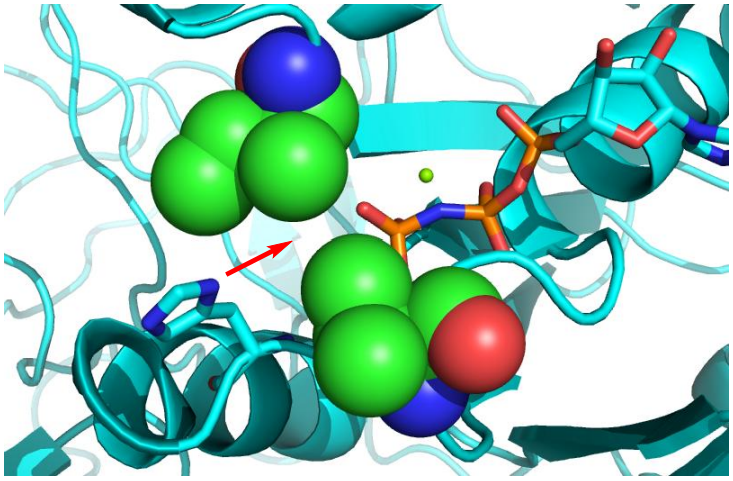

Figure 1.8. Position of His85 and hydrophobic gate. Ile61 and Val20 are shown with spheres (PDB ID: 1EFT).

Function of His85 acting as a general base during ribosome induced GTP hydrolysis by EF-Tu has been debated [38, 39] while the importance of His85 is indisputable [40, 41]. It seems that further structural studies and biochemical analysis should be carried out and pH dependency of the GTPase reaction should be examined in detail to precisely solve the hydrolysis mechanism.

1.4. Basic Biochemistry of EF-Tu

The total number of EF-Tu molecules is 8-14 times the number of ribosomes while the amount of EF-Tu is equimolar to the amount of tRNA in the cell [42]. It binds to GDP, GTP and several other guanosine containing polyphosphates namely ppGpp, pppGpp, dGDP, GDPCP and GDPNP. Upon comparison of GDP and GTP affinities, it is shown that the affinity is 100 times higher for GDP than for GTP and this difference is eliminated by the removal of domains 2 and 3 [43]. GDP dissociation from EF-Tu is very slow and

after amino acid delivery, reactivation of EF-Tu is achieved by its guanine nucleotide exchange factor EF-Ts [16].

EF-Tu has a high affinity towards aa-tRNA [44]. aa-tRNAs bind to bacterial EF-Tu with uniform affinities because amino acids with large contribution to binding affinity of EF-Tu are bound to tRNAs with smaller contribution to EF-Tu binding and vice versa, thus ensuring an adequate rate of protein synthesis [45].

1.5. Structure-Function Studies of EF-Tu

Through engineered mutants, structure−function studies have been carried out in order to shed light on the EF-Tu functionality regarding the guanine nucleotide binding and exchange, GTP hydrolysis, conformational switching, tRNA binding, and ribosome binding.

In regard to the mechanism of guanine nucleotide exhange, residues His85 [46], His118 [47] and also the residues in helix D [48] are studied in order to reveal their roles. Additionally, the functions of residues Asp80 and Phe81 of EF-Ts have also been examined [49]. These studies, via mutated residues, suggested that none of the single side chains may be responsible for the 60000-fold acceleration of nucleotide exchange managed by the action of EF-Ts alone, and it is concluded that the mechanism seems to be more complex than the initial predictions done through the structural studies. The main mechanistic debate on GTP hydrolysis or phosphate hydrolysis in general is whether it follows an associative or dissociative pathway (Figure 1.9). The associative pathway can be described by the formation of an intermediate with a penta-coordinated phosphorus atom whereas the dissociative pathway can be described by the formation of a metaphosphate ion as an intermediate.

Mechanism of GTP hydrolysis in the presence or absence of the ribosome has also been another subject of point mutations of EF-Tu. Mutation of His85 to alanine resulted in a 10^5-fold decrease in the rate of ribosome-stimulated GTP hydrolysis [40] which is in compliance with the most recent structural studies of EF-Tu on the ribosome [35]. Pre-steady state kinetic studies of EF-Tu mutants at Gly94 and Gly83 residues are also studied

and shown to provide flexibility around the switch II region which revealed the functional ground behind the strict conservation of these residues. Another study suggested that the P_i release is managed by Gly94 [15] in addition to the conformational switching [50]. Gly83 plays a role during GTP hydrolysis [50] via coordinating the catalytic water molecule and establishing the structural transition required for GTPase activation [35].

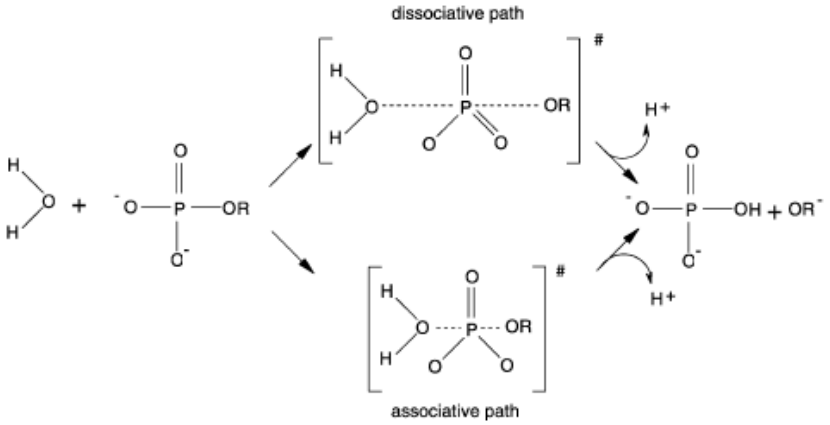

Figure 1.9. Dissociative and associative pathways.

GTP hydrolysis mechanism is proposed to be catalyzed by His85. As suggested for the other G-binding proteins, the reaction is suggested to proceed by a direct in-line attack of a water molecule on the γ-phosphorus atom of GTP. This approach has been examined in a theoretical study [51]. Hypothesizing that His85 would act as a general base, they have calculated energy barriers of GTP hydrolysis in EF-Tu by positioning the His85in ($His85_{in}$) and out ($His85_{out}$) of the active site (Figure 1.10-1.13).

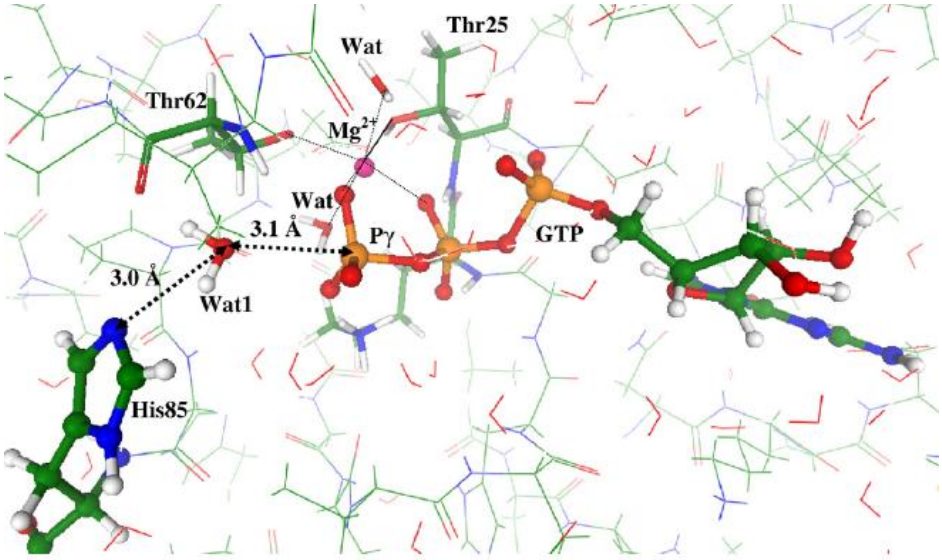

Figure 1.10. Geometry of His85in model at the reactant state [51].

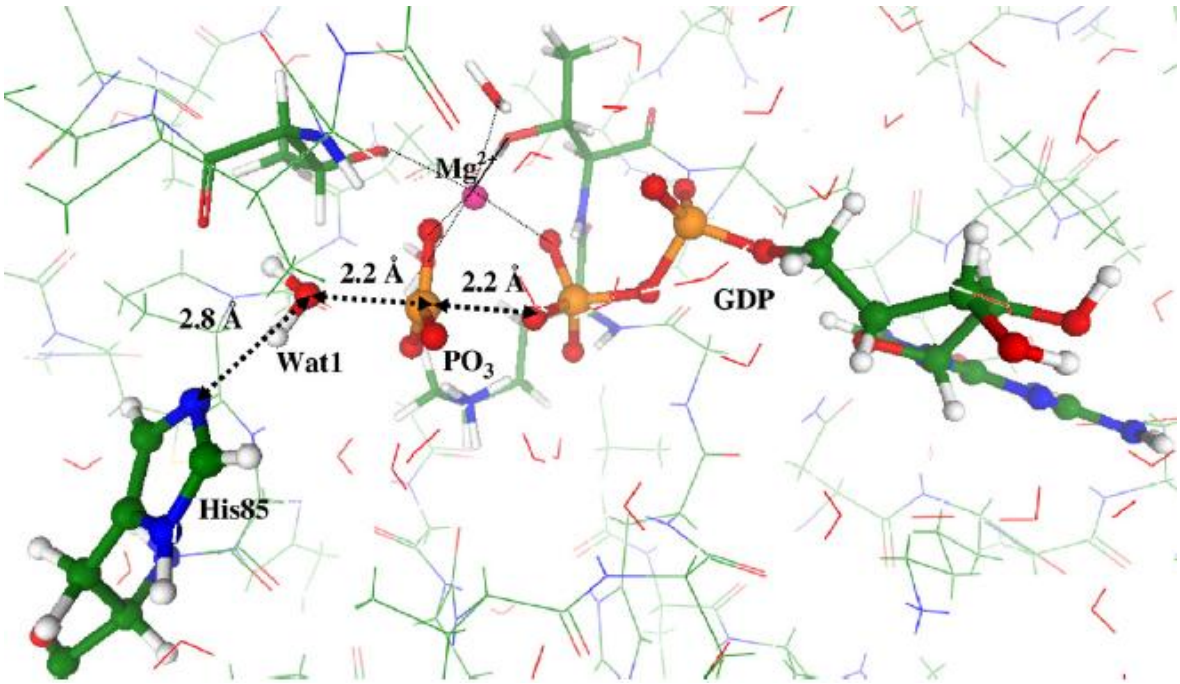

Figure 1.11.Transition state geometry of His85in model [51].

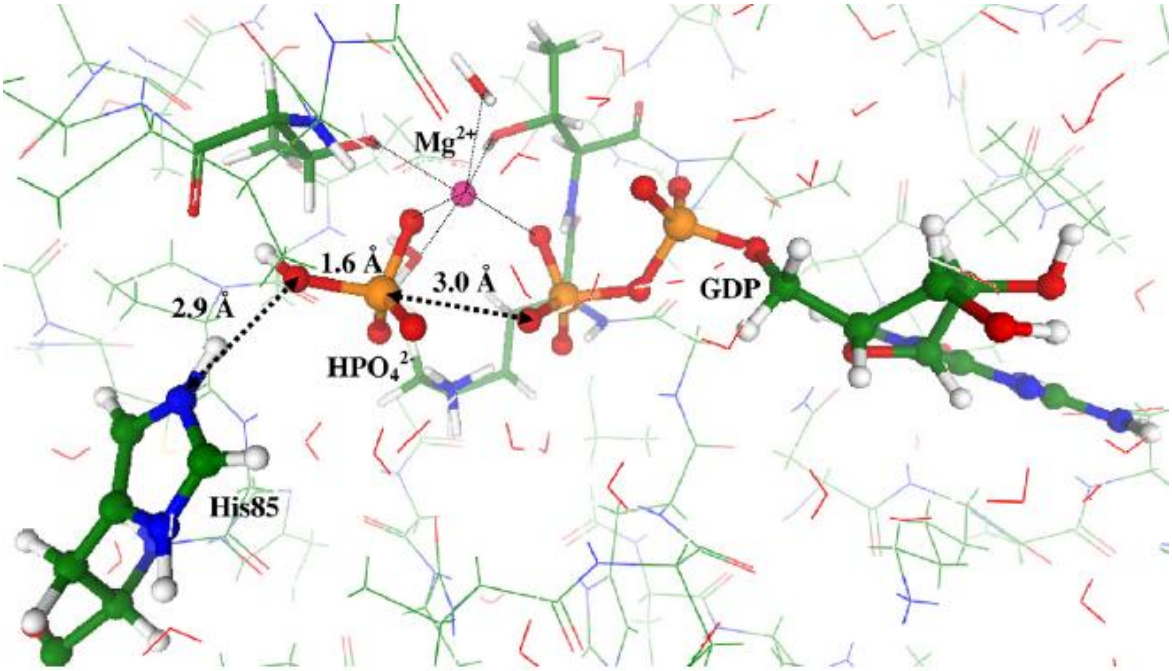

Figure 1.12. Geometry of His85in model, after the hydrolysis [51].

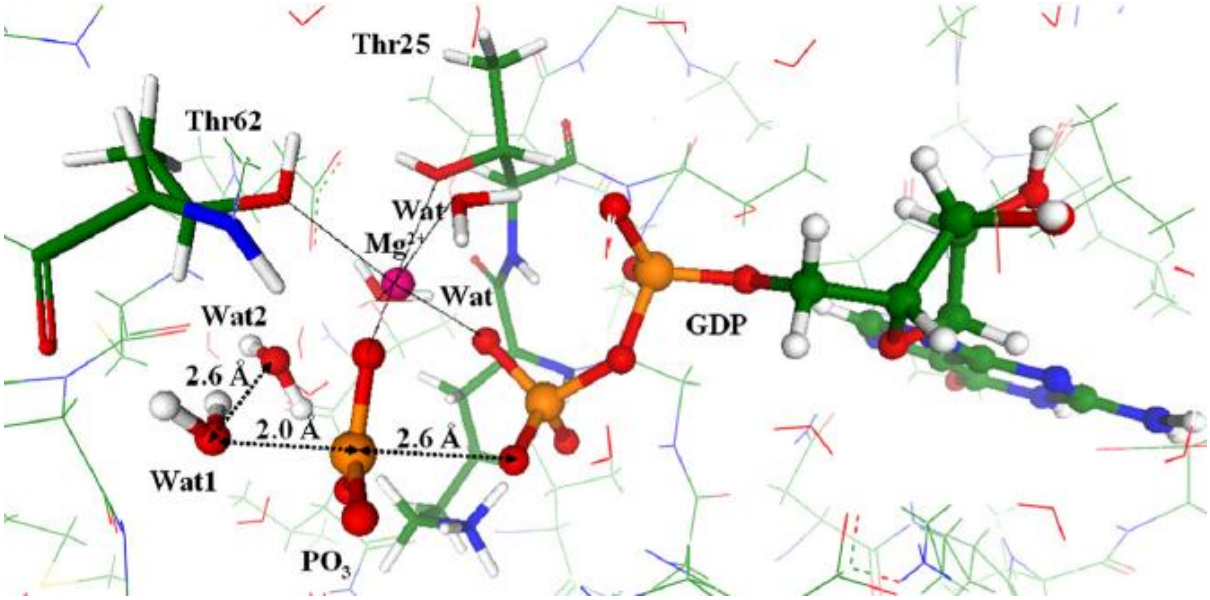

Figure 1.13. Transition state geometry of His85out model [51].

In $His85_{out}$ model, they proposed that an extra water molecule would assist the hydrolysis and with the inclusion of all entropic contributions, GTP hydrolysis activation barrier is calculated to be10.7 kcal/mol and 21.3 kcal/mol for $His85_{in}$ and $His85_{out}$ models,

respectively. Results are in accordance with the standpoint that His85 catalyzes the GTP hydrolysis but consideration of additional factors like ribosome is needed [51].

2. AIM OF THE STUDY

Previously calculations have been carried out on a model system in our group. GTP hydrolysis mechanism is investigated through solvent calculations and transition states for associative and dissociative mechanisms have been located. Based on these studies, we now investigate the nature of the GTP hydrolysis mechanism in EF-Tu·GTP complex from *thermus aquaticus* via QM/MM calculations for a full model. Atoms in the quantum mechanical region are treated with the M062X functional and 6-31+G* basis set using Gaussian09 software while MM atoms are treated with ff03 force field of AMBER.

3. METHODOLOGY

3.1. Force Fields

In the context of molecular mechanics, a force field refers to the functional form and parameter sets used to describe the potential energy of a system of particles (typically but not necessarily atoms). Force field functions and parameter sets are derived from both experimental work and high-level quantum mechanical calculations. A force field is mainly composed of two parts: bonded terms and non-bonded terms. Bond stretching, angle bending and torsion angle can be taken into bonded terms, similarly, van der Waals and Coulomb forces can be taken into non-bonded terms contributions (Figure 3.1).

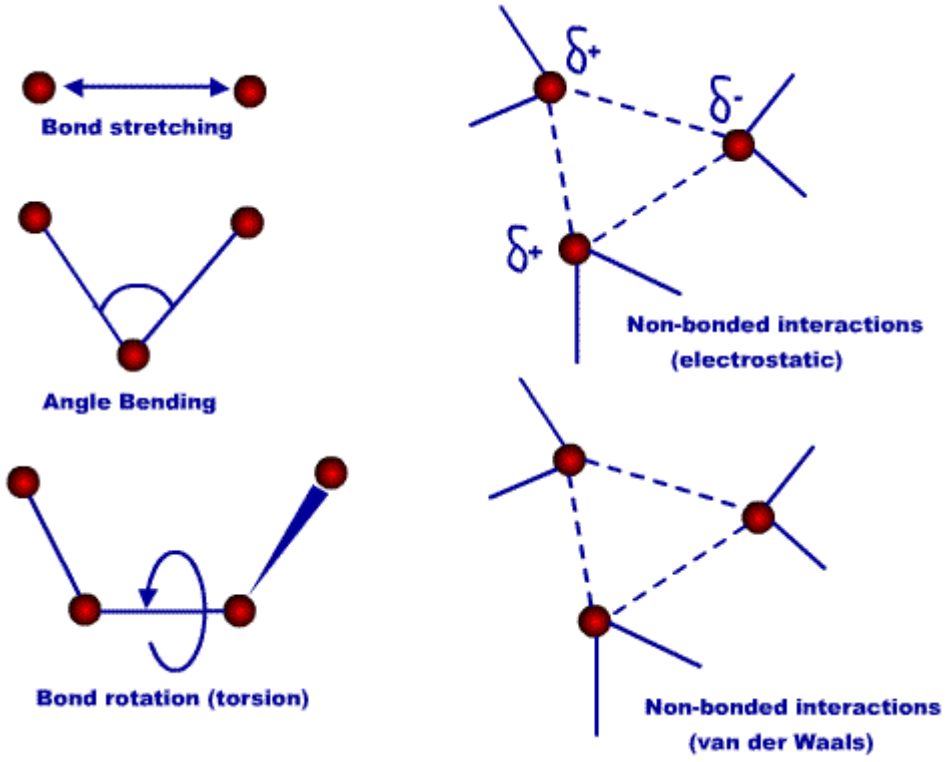

Figure 3.1. Force field contributors.

By using these contributions to the potential energy, E, can be evaluated as follows:

$$E = E_b + E_s + E_\omega + E_{nb} \quad (3.1)$$

E_s is the energy for bond stretching, E_b is the energy for bond angle bending, E_ω is the torsional energy due to twisting about bonds and E_{nb} is the energy for non-bonded interactions. Many different kinds of force-fields have been developed over the years. Some include additional energy terms that describe other kinds of deformations. Some force-fields account for coupling between bending and stretching in adjacent bonds in order to improve the accuracy of the mechanical model.

The design of force-fields for molecular mechanics is guided by the following principles:

(i) Nuclei and electrons are lumped into atom-like particles.
(ii) Atom-like particles are spherical (radii obtained from measurements or theory) and have a partial charge (obtained from theory).
(iii) Interactions are based on springs and classical potentials.
(iv) Interactions parameters must be pre-assigned to specific sets of atoms types.
(v) Interactions determine the spatial distribution of atom-like particles and their energies.

3.1.1. Stretching and Bending

Considering the idea of a molecule to be a collection of masses connected by springs, by applying Hooke's Law we can evaluate the energy required to stretch and bend bonds from their ideal values. Thus E_s and E_b may be expressed as:

$$E_s = \sum_{i=1}^{N} \frac{k_i^s}{2} \left(l - l_0 \right)^2 \tag{3.2}$$

$$E_b = \sum_{i}^{M} \frac{k_i^b}{2} \left(\theta - \theta_0 \right)^2 \tag{3.3}$$

where N is the total number of bonds and M is the total number of bond angles in the molecule. k^s and k^b are the force constants for stretching and bending respectively. l and θ are the actual bond lengths and bond angles. Finally l_0 and θ_0 are ideal bond lengths and bond angles. Unique k^s and l_0 values are assigned to each pair of bonded atoms based on

their types (e.g. C-C, C-H, O-C, etc.). Similarly k^b and θ_0 parameters for angle bending are assigned to each bonded triplet of atoms based on their types (e.g. C-C-C, C-O-C, C-C-H, etc.).

3.1.2. Torsion

The energy due to torsion is usually expressed in terms of a Fourier series,

$$E_\omega = \frac{V_n}{2} \left[1 + \cos\left(n\omega - \gamma\right)\right] \tag{3.4}$$

where the sum is over all unique sequences of bonded atoms. ω is the torsion angle, γ is the phase factor, n is the number of potential energy barriers during a 360 degrees rotation about ω and V_n is the height of these barriers.

3.1.3. Non-Bonded Interactions

The final term contributing to E is the energy from pairwise non-bonded interactions. These interactions are van der Waals and electrostatic interactions.

$$E_{non-bonded} = \underbrace{\sum_i \sum_{j>i} \left(\frac{A_{ij}}{r_{ij}^{12}} - \frac{B_{ij}}{r_{ij}^{6}}\right)}_{\text{van der Waals}} + \underbrace{\sum_i \sum_{j>i} \frac{q_i q_j}{\varepsilon r_{ij}}}_{\text{Coulomb}} \tag{3.5}$$

where the van der Waals interaction between two atoms i and j separated by distance r_{ij} is described by a Lenard Jones potential with parameters A_{ij} and B_{ij}, and a Coulomb potential describes the electrostatic interaction between a pair of atoms i and j using q_i and q_j as partial charges on the atoms and ε as the dielectric constant of the medium.

Usually the parameters for the non-bonded energy terms are obtained by measuring non-bonded contact distances in crystalline hydrocarbons, diamond, graphite and van der Waals contact data for rare gas atoms. Parameters for other atoms are then obtained by extrapolation or interpolation. One major assumption is that the potential derived from

intermolecular interactions can accurately reproduce intramolecular interactions. In addition the interactions are considered to be pairwise additive [52].

An important non-bonded energy term that is always taken into account is the electrostatic interactions. Typically the electrostatic interaction dominates the total energy of a system by a full magnitude. The electrostatic contribution is modeled using a Coulombic potential.

The electrostatic energy is a function of the charge on the non-bonded atoms, their interatomic distance, and a molecular dielectric expression that accounts for the decrease of electrostatic interaction due to the environment (such as by solvent or the molecule itself). A linearly varying distance-dependent dielectric (i.e. 1/r) is sometimes used to account for the increase of ε in environmental bulk as the separation distance between interacting atoms increases. The accuracy of the electrostatic term depends on the correct assignment of charges to individual atoms.

The terms describing energy changes from bond length, bond angle and torsions are well understood and can be accurately included in the overall energy expression. The most influential term, the electrostatic term, however is not fully understood. Hence the variation in the results from different force fields can be attributed, to a large extent, to the electrostatic term. The nature of the parameterizations generating the various force constants and ideal lengths and angles will also affect the applicability of a force field. In general one must consider with which group of molecules or systems a given force field has been parameterized – keeping this fact in mind one may then use the force field on an unknown but similar system. Generality is still a problem with force fields, though with the development of the Universal Force Field (UFF) [53] an attempt has been made to develop a generalized force field applicable to a large portion of the periodic table and not be restricted to particular groupings of atoms such as proteins, nucleic acids etc.

3.2. Hybrid QM/MM methods

It has been known that quantum mechanical methods are widely applicable, require little or no parameterization, and can give very accurate molecular properties, but at large

computational cost. On the other hand, molecular mechanical methods are extremely fast in comparison, and can be used to study very large systems. However, systems of chemical interest are often large (making them difficult for conventional QM treatments) and involve bond breaking or forming processes, highly polar regions, or atom types for which parameterization is difficult.

In many systems the 'difficult' region requiring QM is small, and the majority of atoms in the system are amenable to treatment with MM methods. For example, in many proteins the active site involves only a few residues, and the bulk of the protein, and the surrounding solvent, are not directly involved in chemical reactions or binding (although they still have steric, electronic, and structural effects of course, which must be accounted for). Such systems can be looked at with hybrid QM/MM methods, where the active site is modelled with a QM Hamiltonian, and the surrounding region with a molecular mechanics potential [54]. The two regions interact and influence each other by means of a coupled QM/MM Hamiltonian, as shown in Figure 3.2.

In a QM/MM treatment, the total Hamiltonian is given by:

$$\hat{\mathrm{H}}_{total} = \hat{\mathrm{H}}_{QM} + \hat{\mathrm{H}}_{MM} + \hat{\mathrm{H}}_{QM/MM} \tag{3.6}$$

Here, $\hat{\mathrm{H}}_{\mathrm{QM}}$ is the Hamiltonian of the QM region. $\hat{\mathrm{H}}_{\mathrm{MM}}$ is the energy of the MM region, and $\hat{\mathrm{H}}_{\mathrm{QM/MM}}$ covers the interaction between the two regions, and is defined as:

$$\hat{\mathrm{H}}_{QM/MM} = -\ {}_{e,i}\frac{Q_i}{r_{e,i}} +\ {}_{m,i}\frac{Z_m Q_i}{r_{m,i}} + \hat{\mathrm{H}}_{vdW} \tag{3.7}$$

where *i* is summed over all MM partial charges, *m*over all QM nuclei, and *e*over all QM electrons. The first term gives the one-electron interaction between the QM electron density and the MM partial charges, the second is a standard Coulomb interaction between the QM nuclei and the MM charges, and the final term is a van der Waals interaction term, generally between the QM and MM nuclei. This final term is required since although electron density is explicitly treated in the QM region, it is not in the MM region.

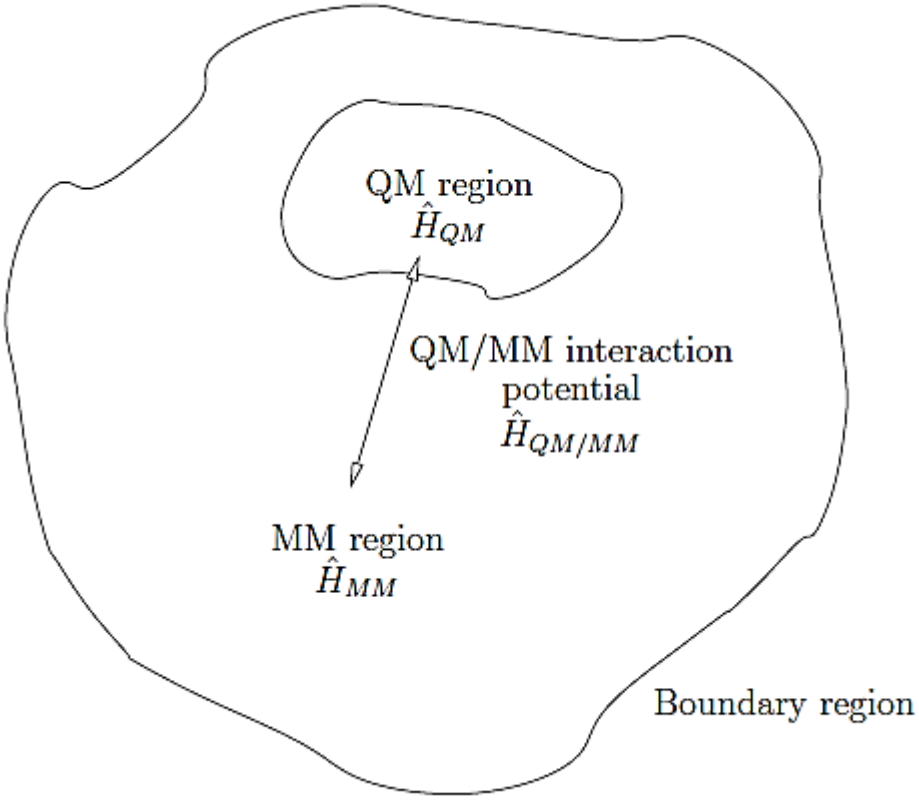

Figure 3.2. The hybrid QM/MM treatment.

Solution of the coupled Hamiltonian gives the total energy as the sum of the energies of the QM and MM systems, and the interaction energy between them:

$$E_{total} = E_{QM} + E_{MM} + E_{QM/MM} \tag{3.8}$$

The energy of interaction between the QM system and a single MM partial charge, Q_i, is then given by:

$$E^i_{QM/MM} = \sum_{\mu} \sum_{\nu} P_{\mu\nu} I^i_{\mu\nu} + \sum_{m} \frac{Z_m Q_i}{r_{m,i}} + E^i_{vdW} \tag{3.9}$$

where $P_{\mu\nu}$ is a density matrix element and $I^i_{\mu\nu}$ a one-electron integral:

$$I^i_{\mu\nu} = -Q_i \int \mu \frac{1}{r_{e,i}} \nu \tag{3.10}$$

The interaction between the QM and MM regions is made more complicated if there are bonds that cross the QM/MM boundary. The electron density of the bond is not properly described, as the QM region lacks the electrons and atomic orbitals of one of the atoms. A number of techniques have been used to treat these bonds. The simplest are perhaps the ‘link atom’ methods, where the QM region is capped with an additional atom (usually hydrogen) which lies on the bond that crosses the boundary. This atom is used to satisfy the valence of the QM region only, and does not usually interact with the MM region. More complex methods such as Generalized Hybrid Orbital (GHO) [55] attempt to optimize the electron density of such frontier bonds for a better join with the MM system. Link atoms and similar methods are vitally important for the simulation of large systems such as proteins, where it is unfeasible to treat the whole molecule with QM.

4. RESULTS AND DISCUSSION

4.1. The Model

In the light of previous studies carried out in our laboratory on EF-Tu, it has been decided to use 4 different geometries of EF-Tu·GTP complex (from *thermus aquaticus:*PDBID:1EFT) in order to investigate GTP hydrolysis mechanisms (associative and dissociative), and to understand the roles of different residues on the hydrolysis mechanisms.

4.1.1. Choice of Initial Geometries

All the structures are taken from the previously performed MD simulations. Main criteria on the choice of initial geometries is the closeness of His85 and Arg57 residues to the active site where GTP is located together with a Mg^{2+} atom in interaction with the O atoms of β-phosphate and γ-phosphate, two water molecules coordinating the Mg^{2+} and p-loop (G_{18}HVDHGKT_{25}) where Asp21, His22, Gly23 and Lys24 is in interaction with GTP through N-terminals and Thr25 directly coordinates with Mg^{2+} atom. Additionally, Thr62 residue also coordinates with Mg^{2+} like Thr25 through the O atom at the side chain. 4 criteria regarding the choice of structures can be listed as:

- His85 in the active site
- Arg57 in the active site
- Both His85 and Arg57 in the active site
- Both His85 and Arg57 out of the active site

Within the chosen residues, His85 has been suggested to serve as a general base in order to deprotonate the catalytic water molecule and initiate its nucleophilic attack to the γ-phosphate of GTP [18, 22, 56]. His85 has also been suggested to orient the attacking water [29] in addition, it may function as a switch with an allosteric effect to shift the p-loop so that the active site conformation is changed to an active state to initiate the hydrolysis of GTP [35]. Arg57 was found to get closer to the active site in the MD

simulations previously performed with ff03 force field with AMBER software in our research group. In order to understand the effect of critical residues, the mechanism should be investigated first in the absence of these residues in the active site. This is the reason why the structure where His85 and Arg57 are out of the active site has been studied. Main focus of this study will be on this structure.

4.1.2. Optimization Strategy

Calculations are performed with ONIOM method of Gaussian09 software. This method basically requires two region definitions; quantum mechanics (QM) region where the atoms will be treated with a QM methodology and molecular mechanics (MM) region which is defined as the rest of the system where atoms are treated with a MM method. In addition to these definitions, a free region also should be defined to select which atoms are allowed to move during optimizations. Using a large QM region and a large free region is problematic because optimizations do not converge. Thus, the size of the QM region and the free region has been increased step by step to achieve convergence.

4.1.2.1. Choice of Functional and Basis Set. In previously performed phosphate hydrolysis calculations on the model system, different functionals have been benchmarked to find the most suitable methodology. With these benchmark studies, the M06-2X functional was found to give the most accurate results. M06-2X is a hybrid meta exchange-correlation and high-nonlocality functional with the double amount of non-local exchange (2X). Its performance is compared to 12 other functionals with 403 energetic data in 29 diverse databases and it is suggested as one of the best functionals together with M05-2X and M06 for a combination of main-group thermochemistry, kinetics, and noncovalent interactions by having the lowest BMUE (Balanced Mean Unsigned Error) [57]. The same functional is preferred for this study as well. In reference to previous studies, the basis set is chosen to be 6-31+G(d) where a polarization function (as a d-orbital) to the heavy atoms is added which gives more room for the electrons to get away from each other to minimize electron-electron repulsion and a diffuse function is also added in s-type and p-type Gaussian on heavy atoms for correct description of weak bonds, especially for H-bonding interactions in our system. For the MM region, the ff03 force field of AMBER is chosen which is also used for the previously performed MD simulations. In order to validate these preferences

for our system, we have also treated our $D51_{in}$ structure with 3 different functionals, namely B3LYP, PBE1PBE and M06-2X and through the preliminary calculations, it is observed that M06-2X/6-31+G(d) method serves best considering the criteria of calculation time, correctly optimized geometries in a chemical point of view and unproblematic convergence.

4.1.2.2. Choice of High Level and Free Region. The free region should be as large as possible to allow critical atoms of the active site move and at the same time it should be as small as possible to prevent undesirable structural rearrangements and decrease the computational time as much as possible without any loss in accuracy. With this information in mind and with the support of a series of calculations, the free region is defined as containing the residues H_{19}VDHGKTT_{26} (magenta color in Figure 4.1), C_{82}PGHADY$_{88}$ (yellow color in Figure 4.1), and G_{60}ITINT$_{65}$ (cyan color in Figure 4.1) in addition to GTP, Mg^{2+}, two water molecules coordinating with the Mg^{2+} and one water molecule in attack position. In our test calculations, it is found that cutting the free region within the peptide bond leads optimization problems since dihedral motion is restricted. Thus, peptide bonds are also defined in the free region by allowing the carbonyl group of next residue to freely move.

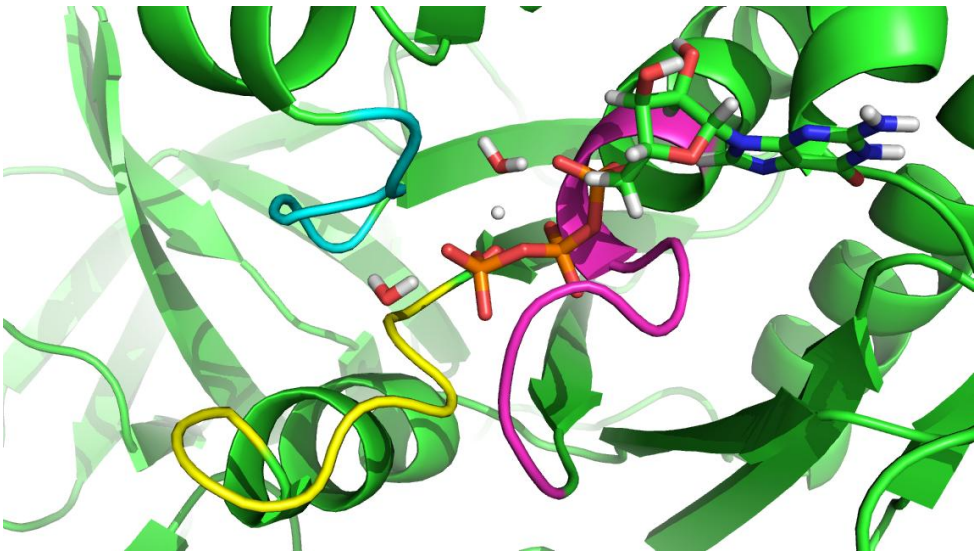

Figure 4.1. Structural representation of free region.

For structure $R57_{in}$ (where Arg57 is close to the active site), additional free region definition is required and for the purpose, Glu56, Arg57 and Ala58 are also added to the free region described above.

Attaining a reasonable high level (QM) region requires careful selection of the atoms considering the computational time and correct representation of the chemical system. In the light of a series of calculations, critically important parts of the system is studied and 4 different QM regions have been chosen, since there are 4 different initial geometries and it is meaningless to use the same definition for each geometry. As a result of these considerations, the QM region of the structure $D51_{in}$ is defined as containing the 3 phosphates of GTP, Mg^{2+}, two coordinating water molecules with Mg^{2+}, attacking water, a part of Thr25 and Thr62 residues, Lys24 residue which directly interacts with O atoms of β-phosphate and γ-phosphate as shown in Figure 4.2 where QM atoms are drawn in red color.

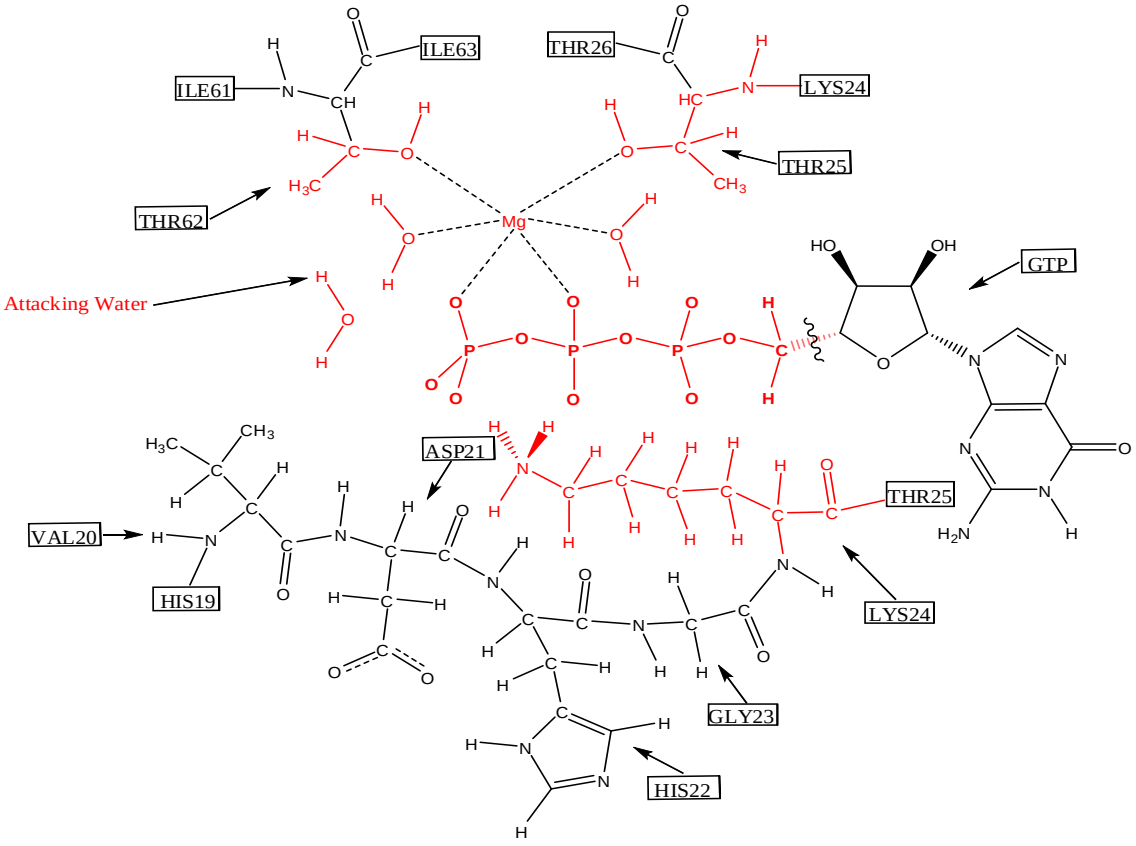

Figure 4.2. QM region defined for D51in.

For the other structures, $R57_{in}$ and $H85_{in}$, the same scheme is used with additional atoms from Arg57 and His85 (Figure 4.3).

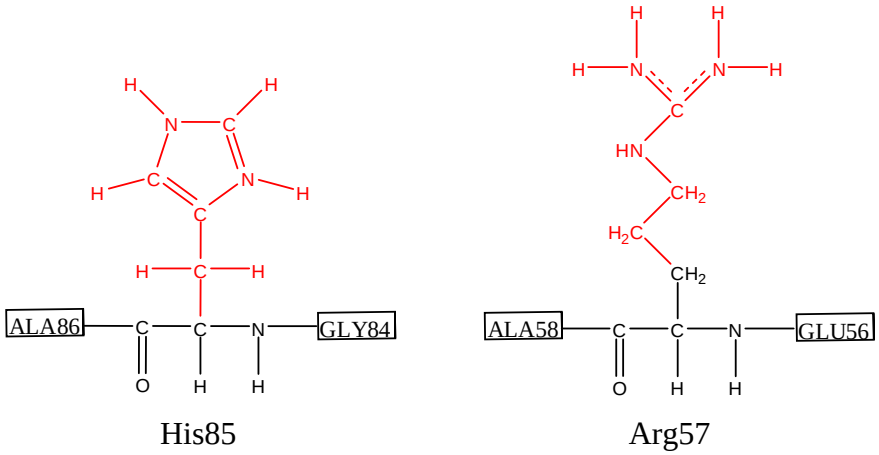

His85 Arg57

Figure 4.3. Additional QM atoms for H85in and R57in structures.

4.2. Reactant Optimizations

In order to understand how critical amino acids affect the hydrolysis pathway, the structure where critical residues are far from the active site should be examined first. For this purpose, a suitable structure is chosen from previously performed MD simulations and treated with QM/MM methodology to converge into the reactant state. The optimized structure and the crystal structure of EF-Tu taken from *thermus aquaticus* [18] are shown in Figure 4.4.

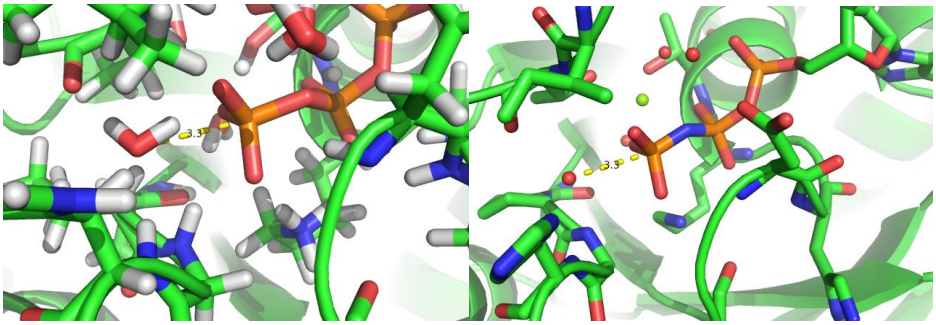

Figure 4.4. Optimized structure and crystal structure (PDBID: 1EFT).

As can be seen from Figure 4.4, the optimized structure and the crystal structure [18] show a great similarity. In both structures, the alignment of p-loop and critical interactions are almost same. In addition, the distance of attacking water to γ-phosphate is same with 3.3 Å. Based on these observations; our starting structure seems geometrically correct in representing the real structure.

4.3. Product Optimizations

It is known from the literature that the product of GTP hydrolysis reaction is an inorganic phosphate ($H_2PO_4^{2-}$) formed by the attacking water and the dissociated γ-phosphate. In order to get insight on the GTP hydrolysis mechanism, it is found worthwhile to investigate possible products of the reaction which also provide valuable information on the transition state path, geometrical orientation of the product in the active site and interactions of protons at the critical region. These calculations are also important to search for the intermediate structure of the dissociative mechanism (P6, P7, P8 and P9 in Figure 4.5). For this purpose, 9 different possibilities are evaluated for structure $D51_{in}$ as shown in Figure 4.5.

After hydrolysis, one of the H atoms of the attacking water should be transferred to an O atom of γ-phosphate or at the end, to β-phosphate. Thus, possible products P1, P2 and P3 are designed based on the location of the hydrogen atom from the water molecule on the inorganic phosphate or β-phosphate. In P1, the hydrogen is located on the inorganic phosphate and it stabilizes the negative charged O atom on the GDP. In P2, the hydrogen atom is located on the negative charged O atom of GDP and it stabilizes the inorganic phosphate through a hydrogen bonding interaction. In P3, the hydrogen is again located on the inorganic phosphate and this time, a proton from Lys24 on the p-loop of EF-Tu is located on the O atom of GDP. These 3 possibilities converge to the same structure which is exactly similar to P1 (Figure 4.6) where the hydrogen atom prefers to stay on the inorganic phosphate rather than GDP and also the proton of Lys24 stays on the lysine rather than migrating to GDP. The distance between the phosphorous atom of the inorganic phosphate and the oxygen atom of GDP is 2.6 Å while the hydrogen bond distance between the inorganic phosphate and GDP is 1.7 Å. On the other hand, the distance between other O atom of GDP and the H atom of Lys24 is 1.5 Å.

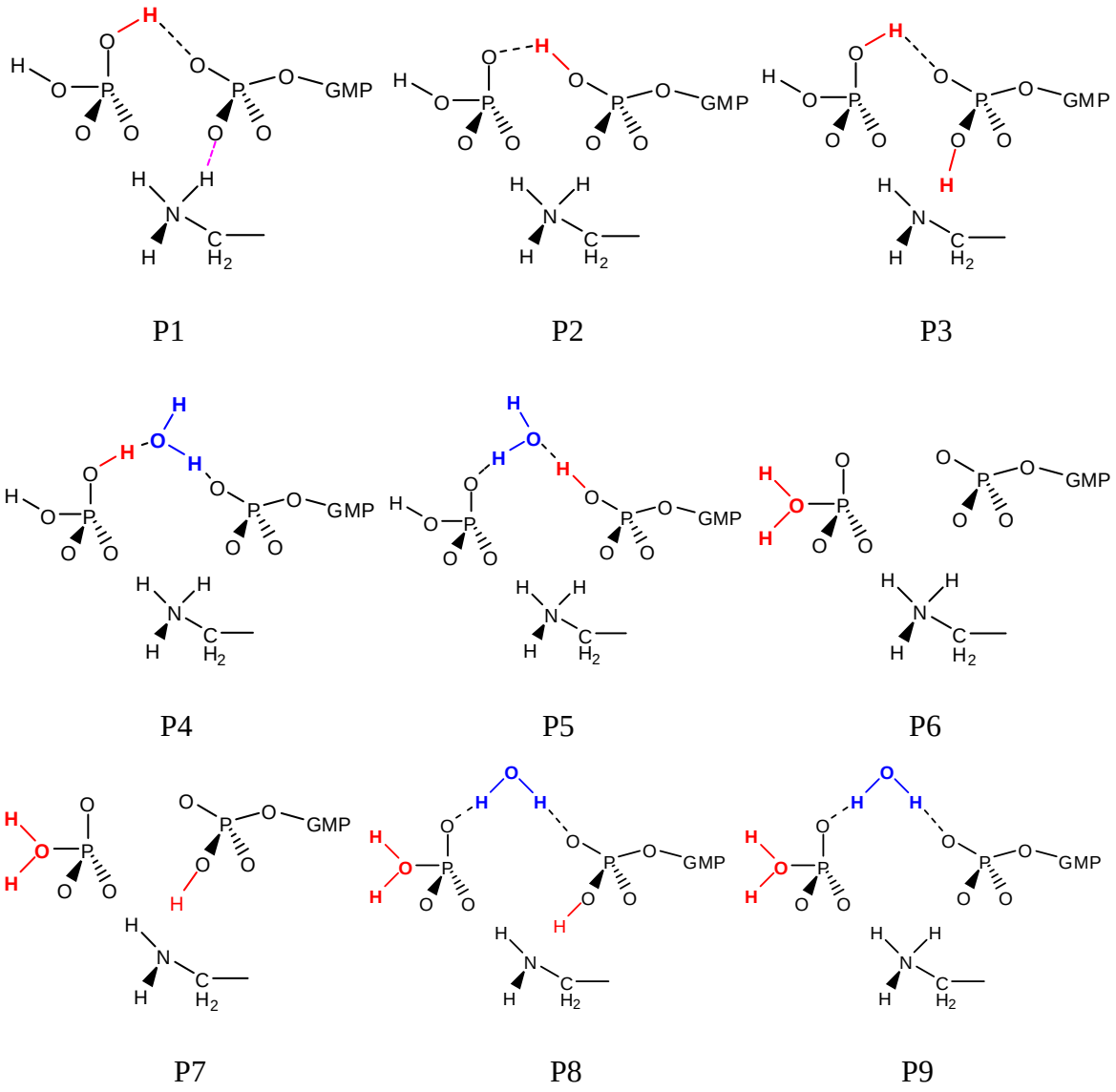

Figure 4.5. Possible products of GTP hydrolysis reaction.

For P4 and P5, one additional water molecule is located between the inorganic phosphate and GDP in order to stabilize the negative charged atoms on these molecules. Within these structures, both possibilities for the location of the H atom are evaluated. The optimized structures are shown in Figure 4.7 and Figure 4.8.

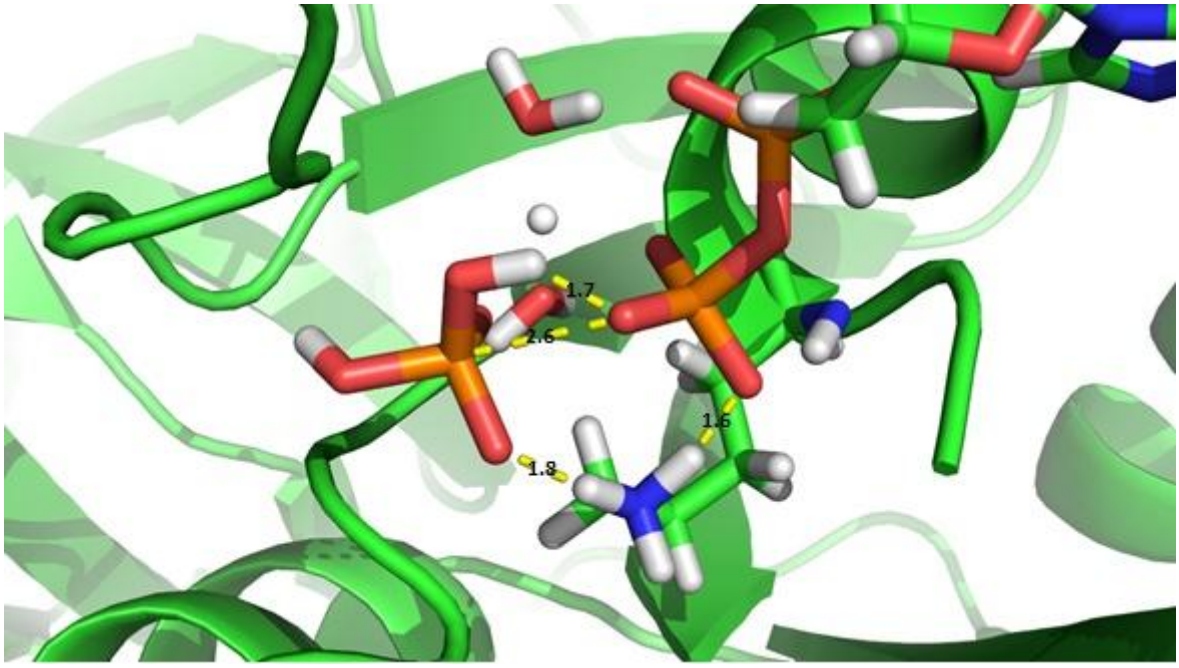

Figure 4.6. Optimized structure of P1, P2 and P3.

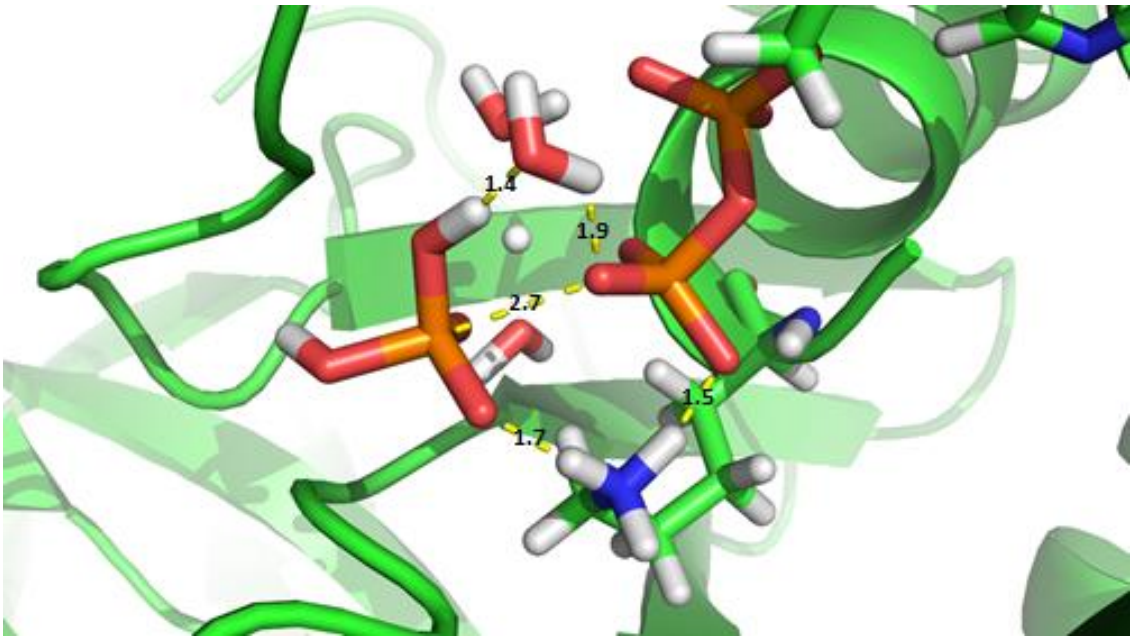

Figure 4.7. Optimized structure of P4.

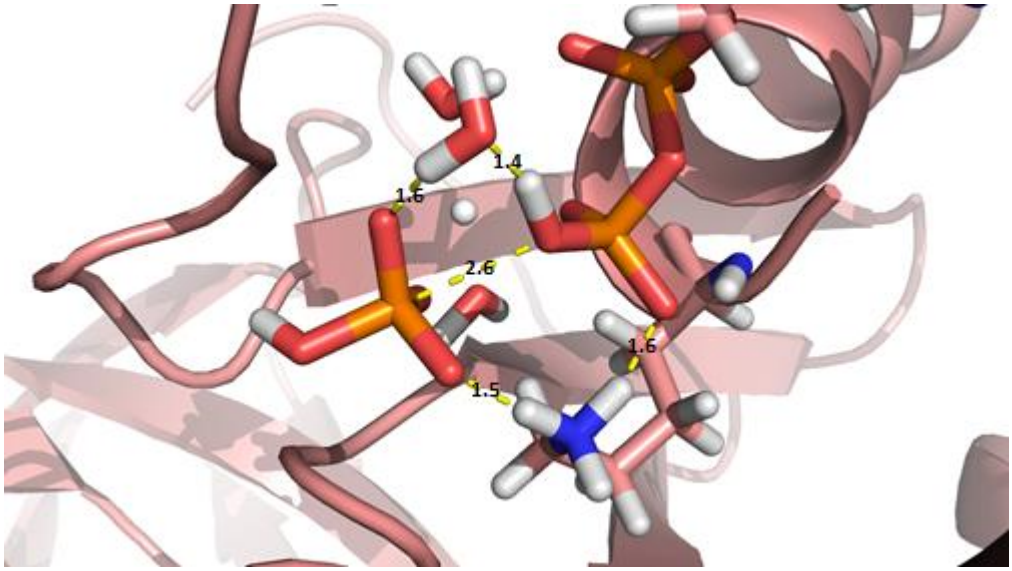

Figure 4.8. Optimized structure of P5.

These calculations reveal that positioning of H atom of Lys24 is influenced by the stabilization of GDP. In P4, bond distance between the Lys24 proton and GDP is 1.5 Å and upon checking P5, this distance is found to be slightly longer as 1.6 Å. The same pattern is valid for the other proton of Lys24 as well. In P5, it is found to be closer (1.6 Å) to the inorganic phosphate than P4 where this distance is 1.7 Å. Thus it can be concluded that Lys24 plays a stabilizing role based on the charge distribution of the products of GTP hydrolysis.

In P6 and P9, where the possibility to form an intermediate product is evaluated, optimizations resulted with the convergence to the reactant state. It can be concluded that there may be no intermediate product as assumed and treated with the structures P6 and P9. This result gives a highly important information since there is no intermediate structure in regard to dissociative mechanism. The dissociative mechanism may not take place at the current geometry where His85 and Arg57 are out of the active site. This does not necessarily mean that there is no dissociative mechanism for the hydrolysis of GTP in EF-Tu since the critical residues are out of the active site and in their presence, this mechanism may be possible. Structures P7 and P8 resulted in a failure to converge. This may be due to the highly unstable initial geometry and H-atom of Lys24 located on GDP in addition to the unstable intermediate product.

Electronic energies of calculations explain the stability of product structures better (Figure 4.9). It is found that P4 is the more stable by 5.0 kcal/mol of energy than P5. P1, P2 and P3 have different reactant states than P4 and P5 so that their energetic data cannot be compared. However, the active site is solvent exposed and it is highly possible for a water to come between inorganic phosphate and GDP with no significant energy cost, so from their energetic data, it may be concluded that an additional water located between inorganic phosphate and GDP stabilizes the structure. Upon comparison of results, it is found that most stable structures are obtained with locating the hydrogen atom from the attacking water on the inorganic phosphate.

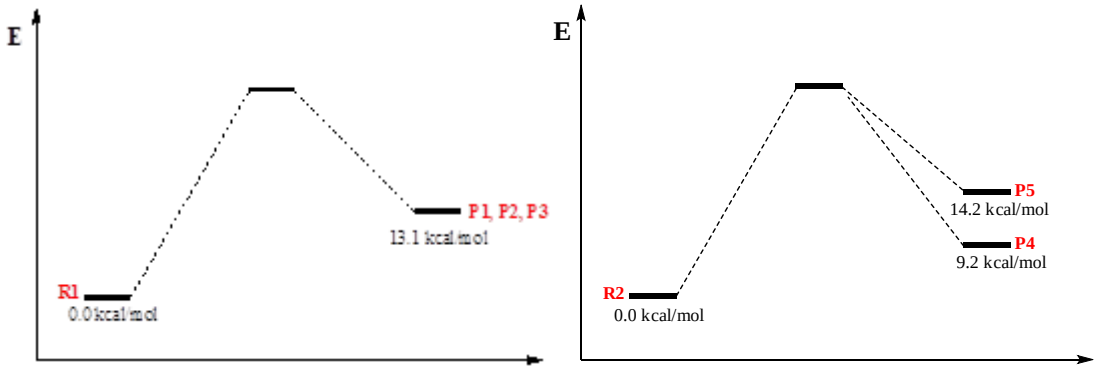

Figure 4.9. Relative energies of P1, P2, P3, P4 and P5.

As a result of product optimizations, it is found that the hydrogen atom coming from the attacking water is situated on the inorganic phosphate and an additional water molecule may be able to stabilize the structure.

4.4. Transition State Optimizations

Reactions needed for the release of inorganic phosphate from EF-Tu•GTP complex consist of 3 steps. At the first step, the enzyme-substrate complex is brought into a reactive state with the rearrangement of the active site. At the second step, a ternary product complex is formed via a chemical transition state (TS). At the third step, the inorganic phosphate (P_i) is released from the system. These steps are shown in Figure 4.10.

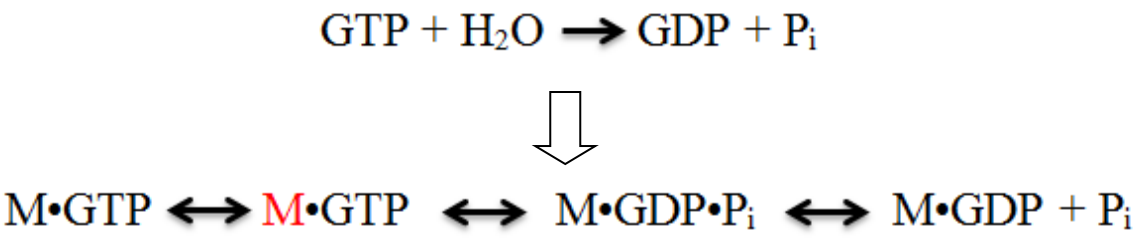

Figure 4.10. General reaction steps of EF-Tu•GTP complex.

At the second step, the transition may proceed via two different pathways. These pathways, debated in the literature, are termed as associative and dissociative pathways. The bond length between the attacking water and γ-phosphate in addition to the distance between γ-phosphate and the β-γ-bridging oxygen is shorter in the associative TS when compared to the dissociative TS. When examined in detail, for the associative TS, it is expected that the attacking water first gives one of its protons to γ-phosphate and then the OH^- attacks the phosphate. In the dissociative mechanism, it is expected that the attacking water and γ-phosphate form an intermediate complex (P6 and P9, Figure 4.5). These mechanisms are shown in Figure 4.11.

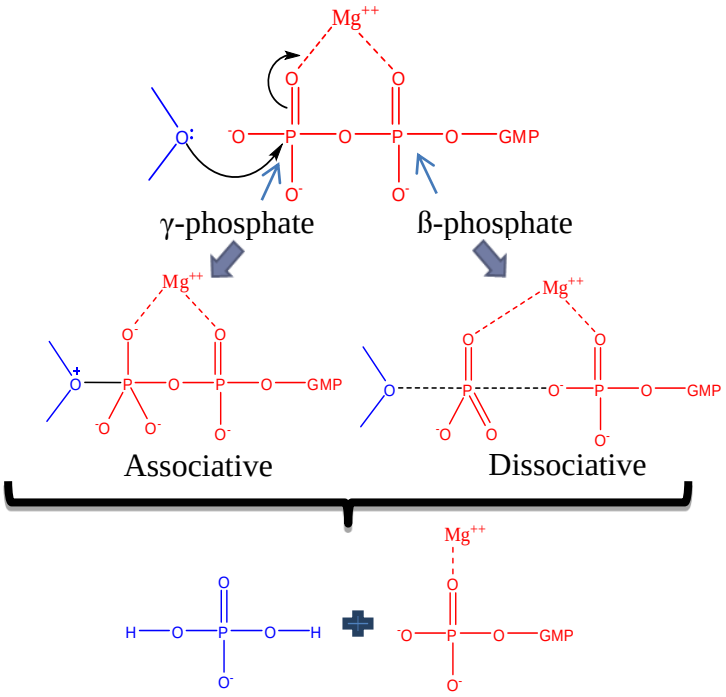

Figure 4.11. GTP hydrolysis mechanisms.

In previous calculations on phosphate hydrolysis performed in our group with a model structure ($CH_3P_2O_7^{3-}$), both associative and dissociative mechanisms have been found as seen in Figure 4.12. The dissociative mechanism has been found to require a lower free energy of activation than associative mechanism by 8.2 kcal/mol. Structural information of these calculations are used as the basis of our studies.

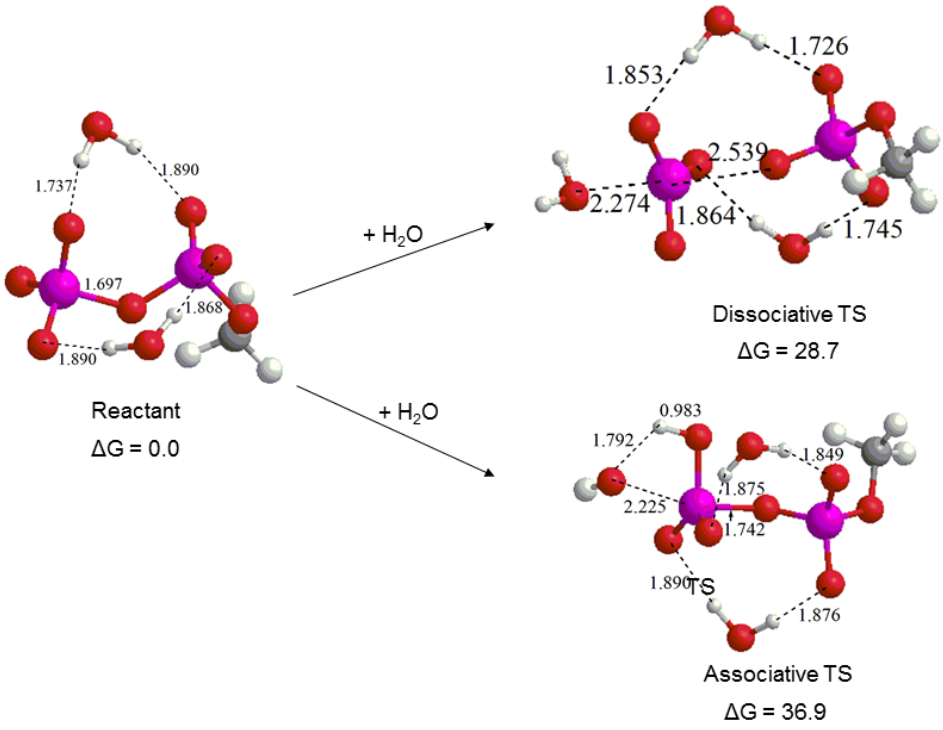

Figure 4.12. Associative TS and Dissociative TS in model structure.

In reference to these calculations, we have aimed to understand the nature of transition state in the absence of critical residues (His85 and Arg57). For this purpose, again $D51_{in}$ structure is used to examine the transition states.

For the associative TS calculation, the initial geometry is prepared by adjusting the γ-phosphate and attacking water distance to 1.8 Å where γ-phosphate and GDP distance is specified to be 1.8 Å as well which is a little longer than the normal covalent bond distance (1.6 Å). Optimization of transition state started with these choices needs 6 criteria to be established for convergence. These criteria are Maximum Force, RMS (Root Mean Square) Force, Maximum Displacement, RMS Displacement, Maximum MM Force and RMS MM

Force. Associative transition state optimizations using the mechanical embedding approach have satisfied all these criteria but optimizations using the electronic embedding approach have satisfied 3 of these criteria (RMS Force, Maximum MM Force and RMS MM Force) after many attempts. During the last steps of the optimizations, the energy and the geometry did not change significantly, therefore we assume that this structure represents the correct result with a very low level of error even though it was not totally converged. Thus it does not constitute any problem at the evaluation of the calculation data. The structure is shown in Figure 4.13.

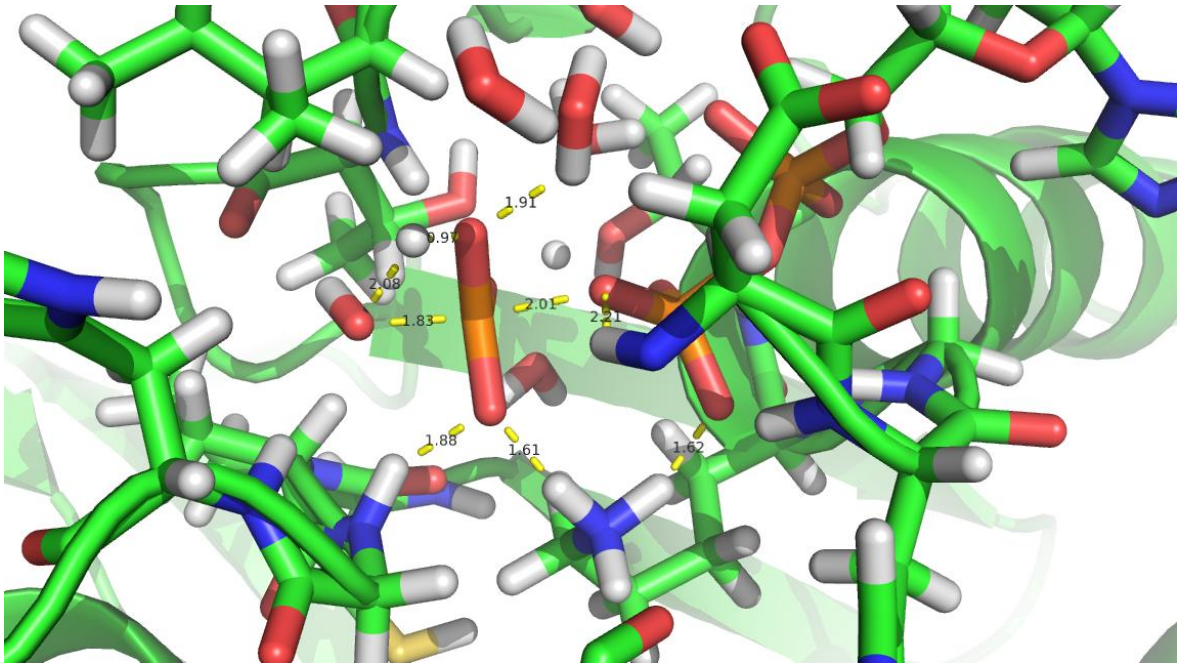

Figure 4.13. Optimized associative transition state geometry.

As can be seen clearly from the figure, one of the protons of attacking water was given to the γ-phosphate. This transfer is in agreement with the observations at product optimizations. PO_3^- is found to form a covalent bond with the proton from attacking water with a distance of 0.97 Å. The negative charge is stabilized by a weak interaction with one of the water molecules with a distance of 1.91 Å. It also has a weak interaction with Thr62 residue. The other O atom is stabilized via interactions with Lys24 residue with a 1.61 Å distance and Gly84 residue with a 1.88 Å distance. The third O atom already keeps its interaction with Mg^{2+} by a 2.05 Å distance and thus stabilizes the negative charge. The hydroxide ion, formed by transferring one of the protons of the attacking water to GTP, is

located at a 1.83 Å distance from the partially positive charged phosphorus which is very close to form a covalent bond.

Upon examining the interactions of β-phosphate, it is observed that γ-phosphate is located at a 2.01 Å distance. At this point, it is seen that Asp21 residue supports the stabilization of the β-γ-bridging oxygen by a 2.21 Å distance. When the other O atom of β-phosphate is examined, it is observed that the negative charge is stabilized via interactions with Lys24, His22, Gly23 and the N-terminal proton of Lys24 at distances of 1.62 Å, 2.29 Å, 2.02 Å and 1.93 Å, respectively. The second O atom is in interaction with Mg^{2+} like γ-phosphate with a 2.06 Å distance.

Barrier of this reaction has been found as 38.2 kcal/mol which is high for the intrinsic GTPase activity. This may be due to the absence of a positive charged residue in the active site such as His85 and Arg57. In the absence of ribosome, His85 in protonated form may be entering the active site from time to time to stabilize OH^- so that reaction barrier may be decreased to a reasonable level. In case EF-Tu is in complex with ribosome, His85 may be staying at the active site more and thus lowering the energy of the barrier to required level.

In order to locate the dissociative TS, we have scanned the critical distances between the P atom of γ-phosphate and the β-γ-bridging oxygen as well as the oxygen atom of the attacking water and the P atom of γ-phosphate. The relationship between these distances and the proposed mechanisms are schematically shown in Figure 4.14.

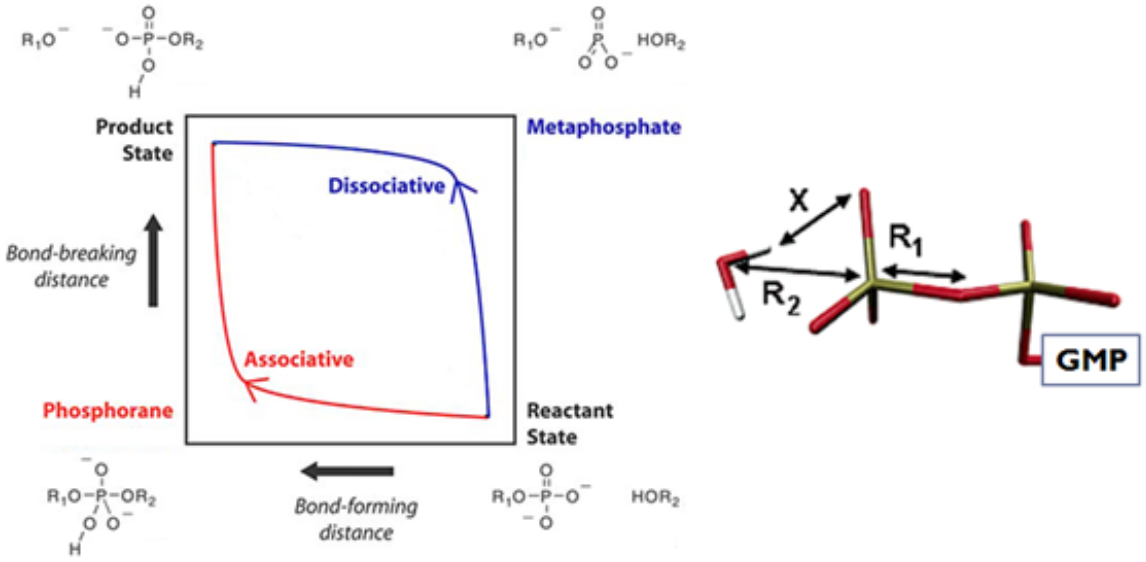

Figure 4.14. Mechanism for phosphate transfer.

For scanning the R_1 and R_2 distances, we have started with R_1 = 2.60 Å and R_2 = 2.20 Å since these distances are thought to represent a structure meeting our dissociative TS description. From this point forward, only 0.1 Å steps are taken and only at one direction by freezing the R_2 and R_1 distances. First, 0.1 Å steps are taken by keeping the R_2 distance constant. Then obtained structures are optimized towards upward and downward directions with 0.1 Å steps meaning that R_2 distance is kept constant and thus only position of water is changed. The relative energies with respect to the reactant's electronic energy are given in Table 4.1.

Orientation of attacking water plays an important role for the dissociative TS. It should be located as one of its lone pairs is targeting and thus interacting with phosphate center. The values written in black in Table 4.1 correspond to the energies calculated when is in this orientation. In this orientation, there will be an unfavorable charge-dipole interaction. Thus charge transfer interactions should be higher to compensate the effect of the unfavorable charge-dipole interaction and make the S_N2 type dissociative mechanism a favorable pathway. The energy should be lowered with the decrease of the forming bond distance. Upon checking the energy values in Table 4.1, it is seen that the energy increases with the decrease of the forming bond distance (R_2) which does not support an S_N2 type

mechanism. This finding is also in agreement with the product calculations since no metaphosphate intermediate has been found.

Table 4.1. Energetic data for dissociative TS pathway (in kcal/mol).

		R_1 distance (in Å)					
		2.20	2.30	2.40	2.50	2.60	2.70
R_2 distance (in Å)	1.70				52.2	53.5	52.7
	1.80			35.8	42.6	44.3	43.8
	1.90		32.8	31.1	36.4	38.4	38.2
	2.00		30.0	31.1	32.2	34.5	34.6
	2.10		26.1	27.6	29.0	30.5	32.0
	2.20	*15.1*	22.8	24.7	26.4	28.1	29.9
	2.30		*13.0*	*15.6*	*15.6*	26.0	28.0
	2.40			*20.4*	*20.4*	*16.6*	*18.9*
	2.50					*22.2*	

In another possible orientation of water, one of its protons make a hydrogen bond with one of the oxygens of γ-phosphate. In this orientation, there is a favorable charge-dipole interaction. However, an S_N2 type reaction is not possible since the water oxygen lone pairs are directed away from the phosphorus atom. On the other hand, one can figure out an S_N1 type reaction. In this mechanism, in a first step, bond breaking would take place without nucleophilic participation of the water molecule. Then, in a second step, the water molecule would reorient and attack the metaphosphate ion (formed in the first step). Structures with this orientation are given in the Table 4.1 in italic. Upon checking the energy values, it is seen that energy increases as the breaking bond distance (R_1) increases. However current data is not sufficient to state if energy will start to decrease with increasing R_1 distance. In order to support a S_N1 type mechanism, there should be a maximum with increasing the breaking bond distance and then it should be possible to observe a second maximum with the decrease of the forming bond distance since product formation will be initiated. In sum, since the relative energies of the structures scanned so far in the S_N1 mechanism are not too high (the highest being 18.9 kcal/mol) one cannot exclude the possibility of a S_N1 type dissociative mechanism but since the scan is not complete and a maximum is not yet found our result are not enough to provide evidence

for its existence. Further studies will be required to observe if there is such a mechanism and extend our findings.

5. CONCLUSIONS

We aimed to investigate the different GTP hydrolysis mechanisms (associative and dissociative) in EF-Tu•GTP complex. For this purpose, we have taken snapshots from the MD simulations which have been previously performed in our group. We have also used data from the phosphate hydrolysis calculations performed on a model system in our group. After reactant optimizations, possible products are examined for $D51_{IN}$ structure to shed light on the transition states. Within these calculations, 9 different possible structures are evaluated including the intermediates of a possible dissociative mechanism. As a result of product optimizations, it is found that hydrogen atom coming from attacking water prefers to stay on γ-phosphate regardless of the additional water molecule and additional water molecule has potential to further stabilize the structure. Then transition state calculations are performed on the $D51_{IN}$ structure in order to understand the nature of the transition state in the absence of critical residues. These calculations gave valuable information on the geometrical rearrangement of active site and critical interactions within the same region. The activation energy of the associative mechanism has been found as 38.2 kcal/mol which is high for the intrinsic GTPase activity. This may be due to the absence of a positive charged residue in the active site such as His85 and Arg57 which may stabilize the OH^- form of attacking water after transferring one of its protons to γ-phosphate. At the evaluation stage of energetic data for searching a dissociative type mechanism, it is seen that energy increases with the decrease of the forming bond distance (R_2) which does not support an S_N2 type mechanism. This finding is also in agreement with the product calculations since no intermediate has been found. On the other side, a possible S_N1 type dissociative mechanism was investigated. No maximum has been found with increasing the breaking bond distance and current data is also insufficient to observe if a second maximum exists with the decrease of the forming bond distance. Further studies are required to support and extend our findings.

REFERENCES

1. Margus, T., M. Remm and T. Tenson, "Phylogenetic Distribution of Translational Gtpases in Bacteria", *Bmc Genomics,* Vol. 8, pp. 1-18, 2007.

2. Maitra, U., E. A. Stringer and A. Chaudhuri, "Initiation-Factors in Protein-Biosynthesis", *Annual Review of Biochemistry,* Vol. 51, pp. 869-900, 1982.

3. Parmeggiani, A. and G. Sander, "Properties and Regulation of the Gtpase Activities of Elongation Factor-Tu and Factor-G, and of Initiation Factor-Ii", *Molecular and Cellular Biochemistry,* Vol. 35, No. 3, pp. 129-158, 1981.

4. Pape, T., W. Wintermeyer and M. V. Rodnina, "Complete Kinetic Mechanism of Elongation Factor Tu-Dependent Binding of Aminoacyl-Trna to the a Site of the E-Coli Ribosome", *Embo Journal,* Vol. 17, No. 24, pp. 7490-7497, 1998.

5. Hilgenfeld, R., "How Do the Gtpases Really Work", *Nature Structural Biology,* Vol. 2, No. 1, pp. 3-6, 1995.

6. Rodnina, M. V. and W. Wintermeyer, "Fidelity of Aminoacyl-Trna Selection on the Ribosome: Kinetic and Structural Mechanisms", *Annual Review of Biochemistry,* Vol. 70, pp. 415-435, 2001.

7. Blanchard, S. C., "Single-Molecule Observations of Ribosome Function", *Current Opinion in Structural Biology,* Vol. 19, No. 1, pp. 103-109, 2009.

8. Zaher, H. S., J. J. Shaw, S. A. Strobel and R. Green, "The 2 '-Oh Group of the Peptidyl-Trna Stabilizes an Active Conformation of the Ribosomal Ptc", *Embo Journal,* Vol. 30, No. 12, pp. 2445-2453, 2011.

9. Rodnina, M. V. and W. Wintermeyer, "The Ribosome as a Molecular Machine: The Mechanism of Trna-Mrna Movement in Translocation", *Biochemical Society Transactions,* Vol. 39, pp. 658-662, 2011.

10. Kavaliauskas, D., P. Nissen and C. R. Knudsen, "The Busiest of All Ribosomal Assistants: Elongation Factor Tu", *Biochemistry,* Vol. 51, No. 13, pp. 2642-2651, 2012.

11. Rodnina, M. V., T. Pape, R. Fricke, L. Kuhn and W. Wintermeyer, "Initial Binding of the Elongation Factor Tu Center Dot Gtp Center Dot Aminoacyl-Trna Complex Preceding Codon Recognition on the Ribosome", *Journal of Biological Chemistry,* Vol. 271, No. 2, pp. 646-652, 1996.

12. Pape, T., W. Wintermeyer and M. Rodnina, "Induced Fit in Initial Selection and Proofreading of Aminoacyl-Trna on the Ribosome", *Embo Journal,* Vol. 18, No. 13, pp. 3800-3807, 1999.

13. Gromadski, K. B. and M. V. Rodnina, "Kinetic Determinants of High-Fidelity Trna Discrimination on the Ribosome", *Molecular Cell,* Vol. 13, No. 2, pp. 191-200, 2004.

14. Gromadski, K. B., T. Daviter and M. V. Rodnina, "A Uniform Response to Mismatches in Codon-Anticodon Complexes Ensures Ribosomal Fidelity", *Molecular Cell,* Vol. 21, No. 3, pp. 369-377, 2006.

15. Kothe, U. and M. V. Rodnina, "Delayed Release of Inorganic Phosphate from Elongation Factor Tu Following Gtp Hydrolysis on the Ribosome", *Biochemistry,* Vol. 45, No. 42, pp. 12767-12774, 2006.

16. Gromadski, K. B., H. J. Wieden and M. V. Rodnina, "Kinetic Mechanism of Elongation Factor Ts-Catalyzed Nucleotide Exchange in Elongation Factor Tu", *Biochemistry,* Vol. 41, No. 1, pp. 162-169, 2002.

17. Rodnina, M. V., K. B. Gromadski, U. Kothe and H. J. Wieden, "Recognition and Selection of Trna in Translation", *Febs Letters,* Vol. 579, No. 4, pp. 938-942, 2005.

18. Kjeldgaard, M., P. Nissen, S. Thirup and J. Nyborg, "The Crystal-Structure of Elongation-Factor Ef-Tu from Thermus-Aquaticus in the Gtp Conformation", *Structure,* Vol. 1, No. 1, pp. 35-50, 1993.

19. Polekhina, G., S. Thirup, M. Kjeldgaard, P. Nissen, C. Lippmann and J. Nyborg, "Helix Unwinding in the Effector Region of Elongation Factor Ef-Tu-Gdp", *Structure,* Vol. 4, No. 10, pp. 1141-1151, 1996.

20. Bourne, H. R., D. A. Sanders and F. Mccormick, "The Gtpase Superfamily - Conserved Structure and Molecular Mechanism", *Nature,* Vol. 349, No. 6305, pp. 117-127, 1991.

21. Kjeldgaard, M., J. Nyborg and B. F. C. Clark, "Protein Motifs .10. The Gtp Binding Motif: Variations on a Theme", *Faseb Journal,* Vol. 10, No. 12, pp. 1347-1368, 1996.

22. Berchtold, H., L. Reshetnikova, C. O. A. Reiser, N. K. Schirmer, M. Sprinzl and R. Hilgenfeld, "Crystal-Structure of Active Elongation-Factor Tu Reveals Major Domain Rearrangements", *Nature,* Vol. 365, No. 6444, pp. 368-368, 1993.

23. Kjeldgaard, M. and J. Nyborg, "Refined Structure of Elongation Factor-Ef-Tu from Escherichia-Coli", *Journal of Molecular Biology,* Vol. 223, No. 3, pp. 721-742, 1992.

24. Nissen, P., M. Kjeldgaard, S. Thirup, G. Polekhina, L. Reshetnikova, B. F. C. Clark and J. Nyborg, "Crystal-Structure of the Ternary Complex of Phe-Trna(Phe), Ef-Tu, and a Gtp Analog", *Science,* Vol. 270, No. 5241, pp. 1464-1472, 1995.

25. Nissen, P., S. Thirup, M. Kjeldgaard and J. Nyborg, "The Crystal Structure of Cys-Trna(Cys)-Ef-Tu-Gdpnp Reveals General and Specific Features in the Ternary

Complex and in Trna", *Structure with Folding & Design,* Vol. 7, No. 2, pp. 143-156, 1999.

26. Kawashima, T., C. BerthetColominas, M. Wulff, S. Cusack and R. Leberman, "The Structure of the Escherichia Coli Ef-Tu Center Dot Ef-Ts Complex at 2.5 Angstrom Resolution", *Nature,* Vol. 381, No. 6578, pp. 172-172, 1996.

27. Wang, Y., Y. X. Jiang, M. MeyeringVoss, M. Sprinzl and P. B. Sigler, "Crystal Structure of the Ef-Tu Center Dot Ef-Ts Complex from Thermus Thermophilus", *Nature Structural Biology,* Vol. 4, No. 8, pp. 650-656, 1997.

28. Stark, H., M. V. Rodnina, J. RinkeAppel, R. Brimacombe, W. Wintermeyer and M. vanHeel, "Visualization of Elongation Factor Tu on the Escherichia Coli Ribosome", *Nature,* Vol. 389, No. 6649, pp. 403-406, 1997.

29. Schmeing, T. M., R. M. Voorhees, A. C. Kelley, Y. G. Gao, F. V. Murphy, J. R. Weir and V. Ramakrishnan, "The Crystal Structure of the Ribosome Bound to Ef-Tu and Aminoacyl-Trna", *Science,* Vol. 326, No. 5953, pp. 688-694, 2009.

30. Li, W., X. Agirrezabala, J. L. Lei, L. Bouakaz, J. L. Brunelle, R. F. Ortiz-Meoz, R. Green, S. Sanyal, M. Ehrenberg and J. Frank, "Recognition of Aminoacyl-Trna: A Common Molecular Mechanism Revealed by Cryo-Em", *Embo Journal,* Vol. 27, No. 24, pp. 3322-3331, 2008.

31. Wimberly, B. T., D. E. Brodersen, W. M. Clemons, R. J. Morgan-Warren, A. P. Carter, C. Vonrhein, T. Hartsch and V. Ramakrishnan, "Structure of the 30s Ribosomal Subunit", *Nature,* Vol. 407, No. 6802, pp. 327-339, 2000.

32. Ban, N., P. Nissen, J. Hansen, P. B. Moore and T. A. Steitz, "The Complete Atomic Structure of the Large Ribosomal Subunit at 2.4 Angstrom Resolution", *Science,* Vol. 289, No. 5481, pp. 905-920, 2000.

33. Yusupov, M. M., G. Z. Yusupova, A. Baucom, K. Lieberman, T. N. Earnest, J. H. D. Cate and H. F. Noller, "Crystal Structure of the Ribosome at 5.5 Angstrom Resolution", *Science,* Vol. 292, No. 5518, pp. 883-896, 2001.

34. Ogle, J. M. and V. Ramakrishnan, "Structural Insights into Translational Fidelity", *Annual Review of Biochemistry,* Vol. 74, pp. 129-177, 2005.

35. Voorhees, R. M., T. M. Schmeing, A. C. Kelley and V. Ramakrishnan, "The Mechanism for Activation of Gtp Hydrolysis on the Ribosome", *Science,* Vol. 330, No. 6005, pp. 835-838, 2010.

36. Jacquet, E. and A. Parmeggiani, "Substitution of Val20 by Gly Elongation-Factor Tu - Effects on the Interaction with Elongation-Factors Ts, Aminoacyl-Transfer Rna and Ribosomes", *European Journal of Biochemistry,* Vol. 185, No. 2, pp. 341-346, 1989.

37. Krab, I. M. and A. Parmeggiani, "Mutagenesis of Three Residues, Isoleucine-60, Threonine-61, and Aspartic Acid-80, Implicated in the Gtpase Activity of Escherichia Coli Elongation Factor Tu", *Biochemistry*, Vol. 38, No. 40, pp. 13035-13041, 1999.

38. Adamczyk, A. J. and A. Warshel, "Converting Structural Information into an Allosteric-Energy-Based Picture for Elongation Factor Tu Activation by the Ribosome", *Proceedings of the National Academy of Sciences of the United States of America*, Vol. 108, No. 24, pp. 9827-9832, 2011.

39. Liljas, A., M. Ehrenberg and J. Aqvist, "Comment on "the Mechanism for Activation of Gtp Hydrolysis on the Ribosome"", *Science*, Vol. 333, No. 6038, pp. 37-37, 2011.

40. Daviter, T., H. J. Wieden and M. V. Rodnina, "Essential Role of Histidine 84 in Elongation Factor Tu for the Chemical Step of Gtp Hydrolysis on the Ribosome", *Journal of Molecular Biology*, Vol. 332, No. 3, pp. 689-699, 2003.

41. Voorhees, R. M., T. M. Schmeing, A. C. Kelley and V. Ramakrishnan, "Response to Comment on "the Mechanism for Activation of Gtp Hydrolysis on the Ribosome"", *Science*, Vol. 333, No. 6038, pp. 37-37, 2011.

42. Furano, A. V., "Content of Elongation-Factor Tu in Escherichia-Coli", *Proceedings of the National Academy of Sciences of the United States of America*, Vol. 72, No. 12, pp. 4780-4784, 1975.

43. Parmeggiani, A., G. W. M. Swart, K. K. Mortensen, M. Jensen, B. F. C. Clark, L. Dente and R. Cortese, "Properties of a Genetically Engineered G-Domain of Elongation Factor-Tu", *Proceedings of the National Academy of Sciences of the United States of America*, Vol. 84, No. 10, pp. 3141-3145, 1987.

44. Louie, A. and F. Jurnak, "Kinetic-Studies of Escherichia-Coli Elongation Factor-Tu-Guanosine 5'-Triphosphate-Aminoacyl-Transfer Rna Complexes", *Biochemistry*, Vol. 24, No. 23, pp. 6433-6439, 1985.

45. Schrader, J. M., S. J. Chapman and O. C. Uhlenbeck, "Tuning the Affinity of Aminoacyl-Trna to Elongation Factor Tu for Optimal Decoding", *Proceedings of the National Academy of Sciences of the United States of America*, Vol. 108, No. 13, pp. 5215-5220, 2011.

46. Schummer, T., K. B. Gromadski and M. V. Rodnina, "Mechanism of Ef-Ts-Catalyzed Guanine Nucleotide Exchange in Ef-Tu: Contribution of Interactions Mediated by Helix B of Ef-Tu", *Biochemistry*, Vol. 46, No. 17, pp. 4977-4984, 2007.

47. Dahl, L. D., H. J. Wieden, M. V. Rodnina and C. R. Knudsen, "The Importance of P-Loop and Domain Movements in Ef-Tu for Guanine Nucleotide Exchange", *Journal of Biological Chemistry*, Vol. 281, No. 30, pp. 21139-21146, 2006.

48. Wieden, H. J., K. Gromadski, D. Rodnin and M. V. Rodnina, "Mechanism of Elongation Factor (Ef)-Ts-Catalyzed Nucleotide Exchange in Ef-Tu - Contribution of Contacts at the Guanine Base", *Journal of Biological Chemistry,* Vol. 277, No. 8, pp. 6032-6036, 2002.

49. Zhang, Y. L., X. Li and L. L. Spremulli, "Role of the Conserved Aspartate and Phenylalanine Residues in Prokaryotic and Mitochondrial Elongation Factor Ts in Guanine Nucleotide Exchange", *Febs Letters,* Vol. 391, No. 3, pp. 330-332, 1996.

50. Knudsen, C., H. J. Wieden and M. V. Rodnina, "The Importance of Structural Transitions of the Switch Ii Region for the Functions of Elongation Factor Tu on the Ribosome", *Journal of Biological Chemistry,* Vol. 276, No. 25, pp. 22183-22190, 2001.

51. Grigorenko, B. L., M. S. Shadrina, I. A. Topol, J. R. Collins and A. V. Nemukhin, "Mechanism of the Chemical Step for the Guanosine Triphosphate (Gtp) Hydrolysis Catalyzed by Elongation Factor Tu", *Biochimica Et Biophysica Acta-Proteins and Proteomics,* Vol. 1784, No. 12, pp. 1908-1917, 2008.

52. Boyd, D. B. and K. B. Lipkowitz, "Molecular Mechanics - the Method and Its Underlying Philosophy", *Journal of Chemical Education,* Vol. 59, No. 4, pp. 269-274, 1982.

53. Rappe, A. K., C. J. Casewit, K. S. Colwell, W. A. Goddard and W. M. Skiff, "Uff, a Full Periodic-Table Force-Field for Molecular Mechanics and Molecular-Dynamics Simulations", *Journal of the American Chemical Society,* Vol. 114, No. 25, pp. 10024-10035, 1992.

54. Warshel, A. and M. Levitt, "Theoretical Studies of Enzymic Reactions - Dielectric, Electrostatic and Steric Stabilization of Carbonium-Ion in Reaction of Lysozyme", *Journal of Molecular Biology,* Vol. 103, No. 2, pp. 227-249, 1976.

55. Garcia-Viloca, M. and J. L. Gao, "Generalized Hybrid Orbital for the Treatment of Boundary Atoms in Combined Quantum Mechanical and Molecular Mechanical Calculations Using the Semiempirical Parameterized Model 3 Method", *Theoretical Chemistry Accounts,* Vol. 111, No. 2-6, pp. 280-286, 2004.

56. Eccleston, J. F. and M. R. Webb, "Characterization of the Gtpase Reaction of Elongation-Factor Tu - Determination of the Stereochemical Course in the Presence of Antibiotic-X5108", *Journal of Biological Chemistry,* Vol. 257, No. 9, pp. 5046-5049, 1982.

57. Zhao, Y. and D. G. Truhlar, "The M06 Suite of Density Functionals for Main Group Thermochemistry, Thermochemical Kinetics, Noncovalent Interactions, Excited States, and Transition Elements: Two New Functionals and Systematic Testing of Four M06-Class Functionals and 12 Other Functionals", *Theoretical Chemistry Accounts,* Vol. 120, No. 1-3, pp. 215-241, 2008.